Experimental Investigation of Dither Control on Effective Braking Torque

A Thesis
Presented to
The Academic Faculty

By
Jeff Badertscher

In Partial Fulfillment
Of the Requirements for the Degree
Master of Science in Mechanical Engineering

Georgia Institute of Technology
August 2005

Experimental Investigation of Dither Control on Effective Braking Torque

Approved by:

Dr. Kenneth A. Cunefare
School of Mechanical Engineering
Georgia Institute of Technology

Dr. Al Ferri
School of Mechanical Engineering
Georgia Institute of Technology

Dr. Christopher Lynch
School of Mechanical Engineering
Georgia Institute of Technology

Date Approved: May 5, 2005

ACKNOWLEDGEMENTS

Thank you to Dr. Christopher Lynch and Dr. Al Ferri for agreeing to be on my thesis reading committee. Many thanks to my lab mates for providing assistance in learning all the equipment and software and putting up with the excessive noise. Thank you to Dr. Kenneth A. Cunefare for introducing me to the area of acoustics and leading me through the perils of experimental research.

TABLE OF CONTENTS

LIST OF TABLES

LIST OF FIGURES

CHAPTER 1

INTRODUCTION

The objective of this thesis was to determine the effect of normal dither control on the braking torque in an automotive disc braking system. Dither control is an active, open loop control technique that has been proven to suppress automotive brake squeal [1]. Brake squeal is a friction-induced vibration of braking components resulting in a high frequency (>1000 Hz) audible response. These audible vibrations have caused the automotive industry to spend hundreds of millions of dollars annually in warranty claims [2]. Dither control is thought to suppress brake squeal by averaging out the nonlinearities in the braking system that cause the instability responsible for brake squeal. While dither control's effectiveness has been established, the effect of this control technique on braking performance has not been investigated.

Chapter one provides fundamental information on automotive disc brakes, theories regarding the origin of brake squeal, friction models used to predict the behavior of automotive disc brakes, theories as to the cause of brake squeal, theories of suppressing the brake squeal phenomena and the motivation for this research. Chapter two contains a detailed description of the brake dynamometer, control system, dither implementation system, experimental transducers and data acquisition systems used in this research. Chapter three presents the experimental methodology used to isolate the effect of dither control on braking torque and outlines the statistical analysis used to examine the results. Chapter four presents the experimental results and Chapter five discusses the significance of these findings.

1.1 Automotive Disc Brakes

Figure 1 displays a typical automotive disc brake assembly where the brake torque is transferred to the rotor from the pads to the support plate and then onto the steering knuckle and front suspension. An explanation of the components of a common automotive disc brake system is necessary to understand the orgin of brake squeal.

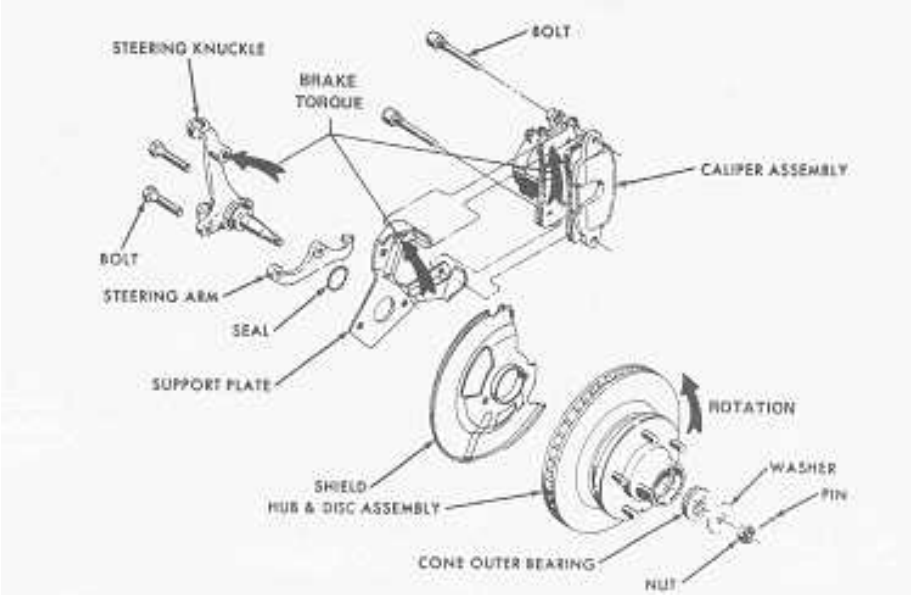

Figure 1 Automotive Disc Brake System [3]

A brake caliper is the casting that is mounted over the rotor and houses the brake pads and hydraulic piston. It must be strong enough to transmit the high clamping forces needed to transfer the braking torque from the pads to the steering knuckle. A 'floating' caliper brake system is used for this research. Figure 2 is a schematic of a floating caliper disc brake. The action of the piston puts pressure on the inboard pad while the caliper reaction puts pressure on the outboard pad. This design ensures that the brake pressure is equally distributed between the two brake pads.

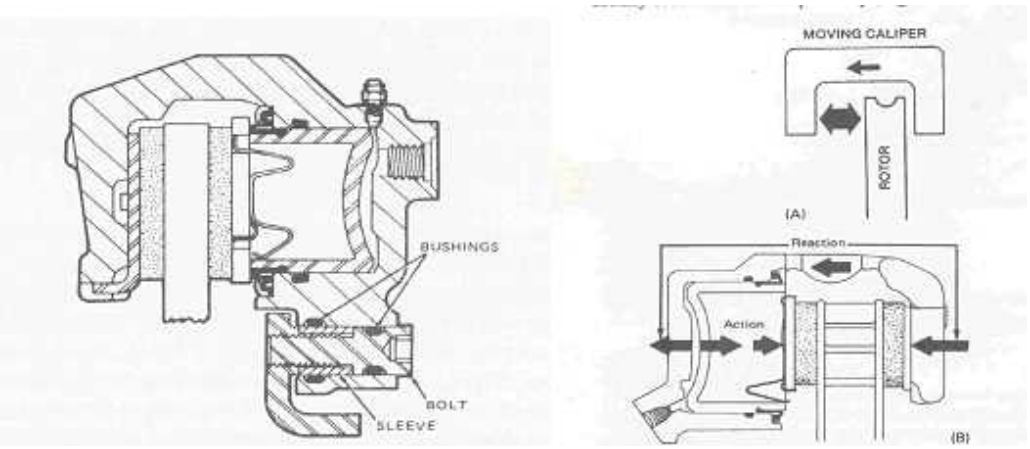

Figure 2 Floating Caliper Disc Brake [3]

1.2 Brake Squeal Theory

Brake squeal is defined to be a high frequency (>1000 Hz) audible vibration of braking components. Brake squeal is generally thought of as the most prevalent and the most objectionable brake noise to passengers and passersby. Many manufacturers of brake pad materials spend up to 50% of their engineering budgets on noise, vibration and harshness issues [4]. There are many published theories as to the exact cause of brake squeal but no consensus as to the precise nature of the brake squeal phenomenon.

A prominent theory used in many approaches is the idea of the brake pad and rotor continually exhibiting a sticking and slipping cycle during braking. Termed by most as the 'stick-slip' phenomenon, it causes the system to exhibit self-excited oscillations. There are several theories as to why the system exhibits this behavior. One theory is that the system has a coefficient of friction that decreases with increasing sliding velocity. Effectively, this property gives a negative damping coefficient and causes unstable oscillations. A simplified model used to describe the 'stick-slip' condition is a friction oscillator, shown in Figure 3. Initially, the slider is stuck on the moving surface.

Eventually, the spring force will be large enough to put the slider into motion. This condition continues until the slider's velocity reaches the surface velocity, where-by the process repeats.

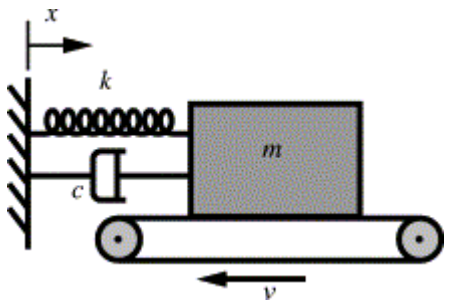

Figure 3 Single Degree of Freedom Friction Oscillator [4]

A similar explanation of a 'stick-slip' condition arises from Spurr's 'sprag-slip' theory. Spurr's theory allows for the assumption that the coefficient of friction is independent of the sliding velocity. A simple model shown in Figure 4 demonstrates the system components oriented in such a way as to increase the normal force until these components deform and slip loose, thus returning to their original position where the process repeats.

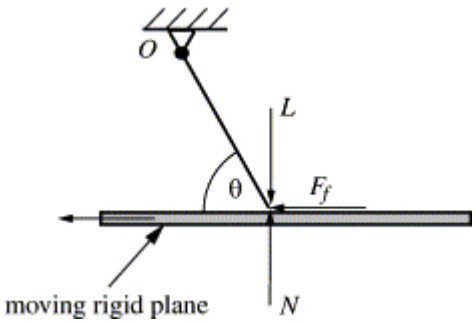

Figure 4 Spurr's Sprag Slip Model [4]

Ouyang *et al*. investigated the vibration of an in-plane slider system on an elastic disc, shown in Figure 5, which demonstrates the 'stick-slip' theory. As the drive point,

which is connected to the slider-mass through an in-plane, elastic spring and damper, is rotated at a constant angular speed around the disc, the driven slider undergoes stick-slip oscillations [5]. This arrangement is considered a model of an automotive disc brake, where the resilience and dissipation of the pad material and the pad support structure are modeled simply by in-plane and transverse springs and dampers. This reduces the brake assembly to a six degree-of-freedom model. The analysis of this system leads to the conclusion that small normal pressures lead to periodic solutions, but the vibrations become unstable at certain large pressures. A similar situation occurs as the drive point rotation speed is increased. Damping from the disc or slider in transverse directions can effectively reduce the magnitude of vibrations and can have a stabilizing effect on an unstable vibration. Damping from the longitudinal direction also reduces the magnitude of vibration but does not have the same stabilizing effect. Similar effects are seen by varying the system stiffness in each direction with only the transverse direction having the stabilizing effect on the system.

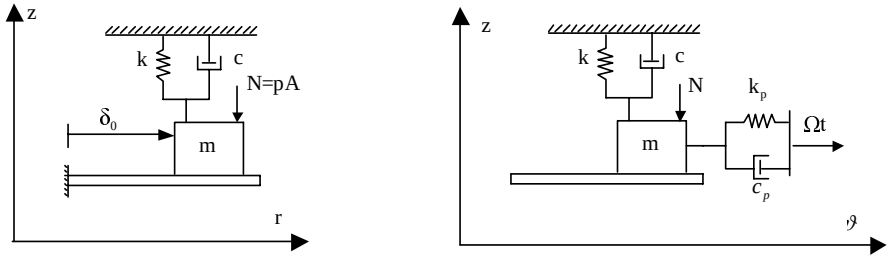

Figure 5 Six Degree-of-Freedom Slider System and Disc in Cylindrical Co-ordinate System used to Demonstrate 'Stick-slip' Oscillations [5]

Matsuzaki *et al*. provided an alternative explanation of squeal generation. Squeal noise tests were conducted with a full sized noise dynamometer utilizing numerous combinations of braking components. Squeal was generated at frequencies of 8.5, 12.8 and 17.7 kHz [6]. These noise tests were repeated while matching different sets of

braking components to determine which of the braking components contributed to the squealing phenomenon. The individual squealing frequencies were found to be more dependent on the brake rotor than any other braking component. Measurements of the natural frequencies of the rotor were carried out to identify the correlation between the squeal frequency and the natural frequencies of the rotor. Figure 6 shows a plot of the natural frequencies of the rotor for the transverse and longitudinal directions, where the longitudinal direction represents the expansion and contraction in the direction of the thickness with the in-board and out-board rotor surfaces having opposite phase. The squeal frequencies correlated with the second, fourth and sixth longitudinal modes of the rotor. This correlation was confirmed when an acoustic intensity analysis mapped the acoustic emission to the mode shapes of these longitudinal modes. This research confirms the existence of audible squeal due to longitudinal vibration of the rotor and provides a valuable alternate explanation of squeal generation.

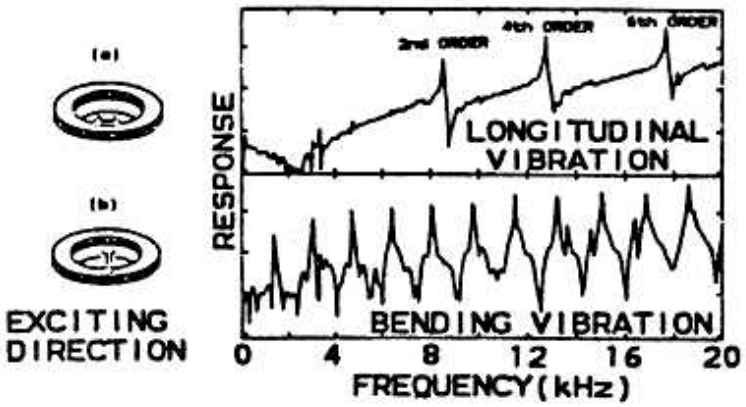

Figure 6 Experimentally Determined Natural Frequencies of the Rotor in Longitudinal and Transverse (bending) Directions [6]

Tuchinda *et al*. contend that there is an onset of a system instability caused by the combination of two vibration modes of the system, termed mode ‘lock-in’ [7]. In their

research, a pin-on-disc system, composed of a flexible pin and flexible disc, is used with a simple Coulomb type friction interaction. Figure 7 shows the pin-on-disc model used along with a description of the displacement coordinates at the pin tip. For their analysis, the first five axial modes and the first five transverse modes of the pin are used, along with the first eighteen modes of the disc. These modes were chosen because they occur at frequencies that fall within the audio frequency range (0 Hz to 16 kHz). Figure 8 shows a plot of the predicted natural frequency (i.e. imaginary parts of eigenvalues) as a function of the coefficient of friction over the frequency band of 500 Hz to 4 kHz [7]. This plot clearly shows the mode lock-in characteristic between the second mode of the pin and the third nodal diameter mode of the disc. With a coefficient of friction of zero both of the eigenvalues for these modes are purely imaginary (real modes). Increasing the coefficient of friction causes the two eigenvalues to approach each other until at a value of 0.27 they coincide and this is the first instance of instability. While the coefficient of friction is between 0.27 and 0.32 the two purely imaginary eigenvalues become two complex eigenvalues, resulting in two complex modes, one of which is stable and one that is unstable.

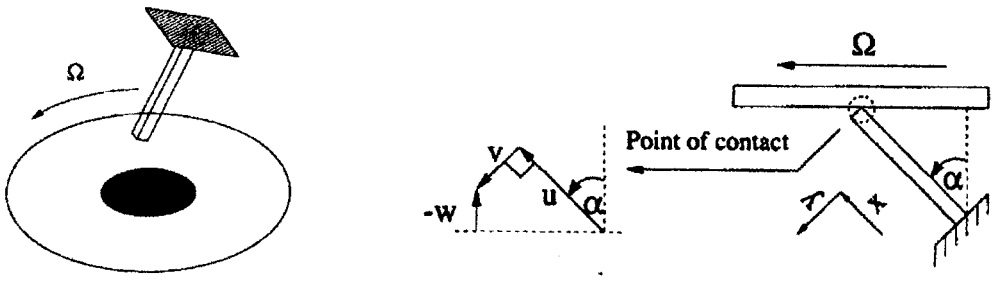

Figure 7 Pin-on-Disc Model with Geometry & Coordinate System [7]

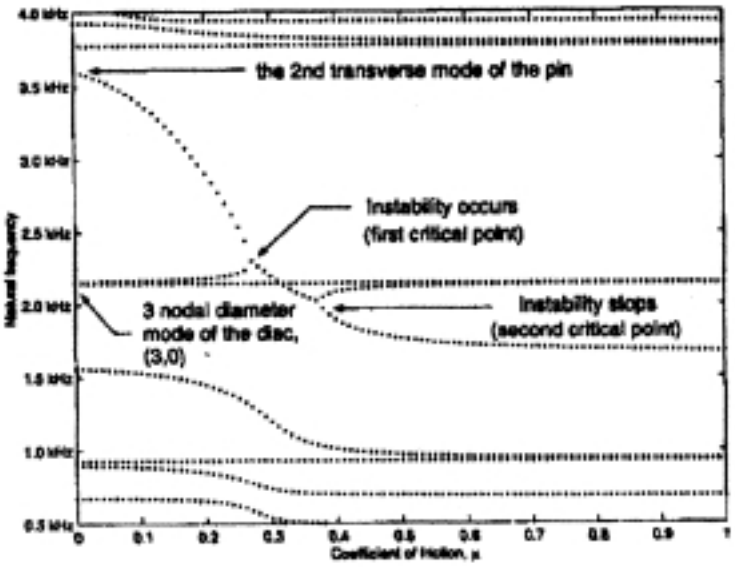

Figure 8 Mode "Lock-In" and "Lock-Out" Characteristics [7]

1.3 Friction Models

A general definition of friction is: when two bodies in contact are subjected to conditions which produce relative sliding motion, friction stresses develop on the interface that tend to oppose that motion. Classic laws of friction that have evolved from early studies according to Moore can be used as a starting point in the discussion of friction [8]. The first classical law states the force due to friction is proportional to the normal contact force, or $|F| = \mu N$, where μ is the coefficient of friction. Most often μ has two values: μ_s, the coefficient of static friction and μ_k, the coefficient of kinetic friction. The coefficient of static friction is used at the onset of sliding and the coefficient of kinetic friction is used during sliding. The second law states that the coefficient of friction is independent of contact area. The third law is that the coefficient of static friction is larger than the coefficient of kinetic friction. The fourth law is that the

coefficient of kinetic friction does not depend on the sliding velocity. The fifth law states that the friction force acts in the direction of tangential motion with the opposite sense. Over the years experimental and theoretical models have challenged these basic laws with varied results. The first two laws are found to hold for gross motions of effectively rigid bodies. The third law is derived from classical experiments using a mass on an inclined plane. The fourth law is invalid, as many experimental and empirical formulas exist demonstrating the variation of the friction coefficient with sliding velocity. The fifth law is valid and confirmed by experiment.

Using a single degree of freedom model with a Hertzian contact stiffness, Hess & Soom investigate the impact of internal and externally applied harmonic and random loads[9-11]. Figure 9 shows the single degree of freedom model used in these investigations. The internally excited case models a rough surface while the externally excited case models the impact of external loads. Both cases are important to understand the impact of additional loads on the mean load using a Hertzian contact stiffness.

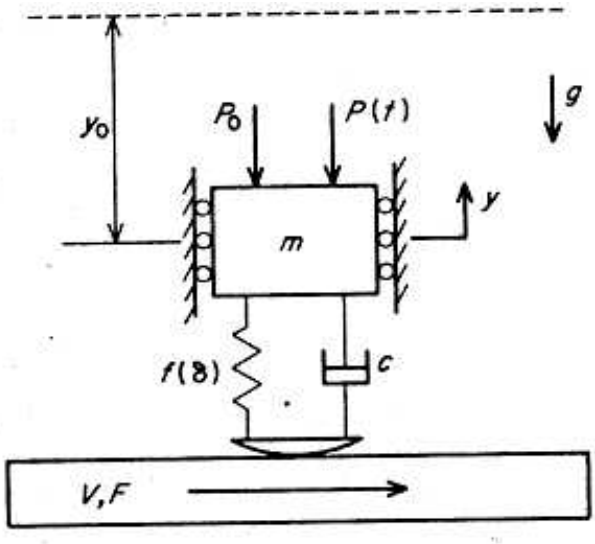

Figure 9 Single Degree of Freedom Model Using a Hertzian Contact Stiffness [9]

Using the aforementioned model and the method of multiple scales the impact of harmonic loading conditions on the mean friction force was quantified by Hess & Soom. The equation of motion governing this system is

$$m\ddot{q}+c\dot{q}-K_1 y_0^{1/2}(1-q)^{3/2}=-\frac{P_0}{y_0}(1+\alpha\cos\Omega t)-\frac{mg}{y_0} \quad \text{where } q=\frac{y}{y_0} \;\&\; y_0=\left(P_0+\frac{mg}{K_1}\right)^{2/3},$$

$$K_1=\frac{4}{3}E'R^{1/2} \;\&\; f(\delta)=K_1\delta^{3/2}.$$

The method of multiple scales is used to solve this non-linear differential equation since the Hertzian system is not highly nonlinear. The frequency investigated in their paper is the region in the neighborhood of the primary resonance of the system.

Using the Hertzian contact theory is it known that the normal elastic contact deflection of a circular contact area is related to the area of contact by $\delta=\frac{A}{\pi R}$. The deflection under the static load, P_0+mg, is $\delta_0=y_0=\frac{A_0}{\pi R}$. Based on the adhesion theory of friction, it is assumed that the instantaneous friction force is proportional to the area of contact. Since the contact deflection is $\delta=y_0-y$, the friction dependence on normal displacement, in terms of average values during steady state vibration, is simply

$$\frac{F_{av}}{F_0}=\frac{A_{av}}{A_0}=1-\frac{y_{av}}{y_0}.$$

This relation allows one to estimate the friction reduction associated with a given average normal displacement [9].

Figure 10 shows the results of a parametric investigation that shows the reduction in friction force is greatest at the primary resonance of the SDOF model and varies

between 1.5% and 10.0%. This loss is associated with the inherent behavior of the Hertzian contact and is independent of the particular loading or contact parameters.

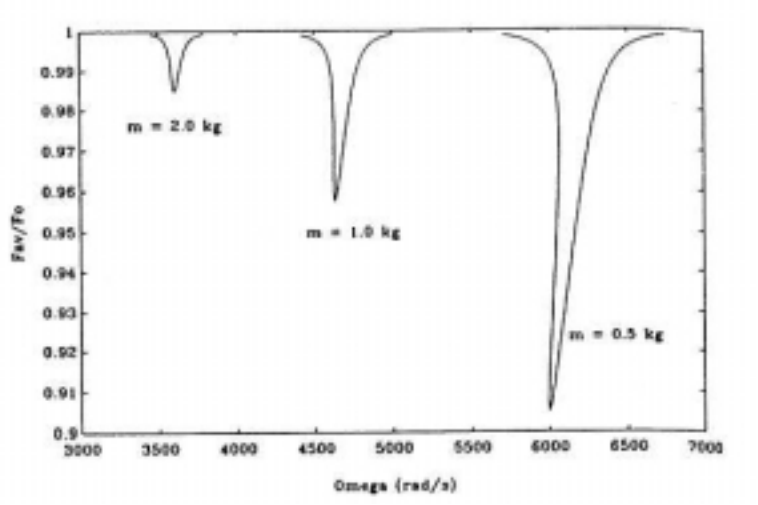

Figure 10 Average Friction for Varying System Mass [9]

Ferri used a single degree of freedom friction oscillator model to demonstrate the possibility that dither has no effect on the average friction force [12]. The equation of motion for the friction oscillator system is

$$m\ddot{x} + c\dot{x} + kx + \mu N \operatorname{sgn}(\dot{x} - v_0) = 0 .$$

When sticking occurs in this system this equation is no longer valid. A simple extension of this equation is to replace the discontinuous sgn function with a steep saturation nonlinearity. A standard Stribeck-type friction model is used to capture the velocity dependence of the friction coefficient. Dither is introduced by letting the normal force vary sinusoidally about the nominal value. In this analysis the average value of the normal load is simply the nominal static pressure force. Thus, for a given relative velocity history, the dither amplitude and frequency have no effect on the average value of the friction force.

Oden and Martins in their investigation into theories to adequately predict stick-slip motion, frictional damping and sliding resistance state that normal vibrations lowers the frictional force because of the inherent nonlinearity in the system [8]. In their work, dynamic friction effects were incorporated into a non-linear continuum model of contact and sliding friction of elastic bodies. The contacting bodies are assumed to be linearly elastic, but the overall theory is highly non-linear, owing to nonlinearities in the contact constraints, frictional behaviors and interface response [8]. They conclude:

> "Contrary to a widely accepted belief that has prevailed since the time of Coulomb, the coefficient of friction may not necessarily change with increasing relative sliding velocity. Our results confirm the experimentally-based conjectures of Tolstoi [13] and some other researchers. This apparent change is traditionally interpreted as a decrease from a static to a kinetic coefficient. It is, however, only the average value of friction force that may decrease after the initiation of sliding and not necessarily instantaneous ratios tangential to normal stress components on the contact surface. Of course, if the sliding body is modeled as a single (tangential) degree-of-freedom system, as is so often the case, then the reduction of the coefficient of friction upon sliding is the only possible device for incorporating these experimentally observed phenomena. Such crude models, experimental and/or analytical, cannot take into account normal force oscillations, and thus omit a critically important property of dynamic friction. Stick-slip motion may be a manifestation of dynamic instabilities inherent in the coupling of normal and tangential relative motions of contacting bodies. This phenomenon is not necessarily the result of a decrease in the coefficient of friction with changes in sliding velocity, and can in fact be observed when the coefficient of friction is constant and equal to its so-called static value" [8].

This work gives an alternative explanation for the reduction of friction force due to the application of a normal dither signal.

1.4 Brake Squeal Suppression

There exists no simple and universal method to eliminate or prevent brake squeal, although various case-by-case remedies have been developed. For squeal caused by longitudinal vibration of the rotor, slotting the rotor suppresses brake squeal [6]. In many

cases vibration shims are applied between the backing plate and the caliper, and in fact many brakes are equipped with these shims at assembly [4]. Other remedies include: chamfering or slotting the friction material, sanding the surface of the brake rotor, applying grease to the piston backing plate and lubricating the pins that connect the caliper to the mounting bracket. The squeal elimination technique investigated in this research is the use of a normal dither signal.

Dither is defined to be a high frequency disturbance used to modify a system's characteristics. Dither control is an open loop control technique. The modern understanding is that dither signals lead to either a reduction of the sector to which the system non-linearity belongs or a relocation of the poles of the system; each of these effects may lead to improvements in system performance [14]. In systems that involve friction, dither is used in order to smooth the "discontinuous" effects of friction at low velocities. Dither can be applied in either the normal or tangential directions. Dither in the tangential direction modifies the influence of friction by its averaging effect while normal dither changes (in mean) the friction coefficient [15].

Normal dither control has been shown experimentally to effectively suppress and prevent rotor mode disc brake squeal. Using the same brake dynamometer and a dither implementation system similar to the one used in this research, dither was shown to eliminate as well as prevent brake squeal from occurring [1, 16]. Cunefare & Graf produced a consistent 5.6 khz squeal for a rotor speed of 54.7 revolutions per minute (rpm), which corresponds to a vehicle speed of 3.5 miles per hour (mph), with a brake line pressure of 0.414 Mpa. Table 1 shows the observed suppression of the squeal response for a variety of dither frequencies.

Table 1 Measured data during brake squeal active control tests [16]

Squeal freq. (kHz)	Squeal level before control (dB)	Dither freq. (kHz)	Squeal level with control (dB)	PZT drive voltage (V rms)	Force on rotor (N rms)	Control signal noise level (dB)
5.6	90	6	55 - 60	143	11.9	90
		7	56 - 60	170	38.3	94
		9	57 - 60	148	11.6	95
		15	58 - 60	95	17.1	85.5
		16	59 - 60	62.3	9.6	88
		18	60 - 60	120	8.9	89
		20	61 - 60	177	10.2	82

Control of the braking system was achieved above an experimentally determined threshold control value [16]. Figure 11 demonstrates the different stages of control. As the dither control amplitude is increased the level of squeal response is diminished until the squeal response is completely removed. This threshold behavior is termed synchronization, a characteristic of dither detailed in the literature [1, 16, 17]. Figure 11a is the sound pressure level during squeal without a dither signal present; the prominent peak is at the 5.6 kHz squeal frequency. Figure 11b presents the sound pressure level after the activation of a 20 kHz, 75 volt rms signal. The 5.6 kHz squeal frequency has been suppressed by approximately 10 dB and a response is present at the 20 kHz dither frequency. Finally, Figure 11c depicts synchronization where the squeal response is suppressed into the noise floor and only the 20 kHz dither response is present.

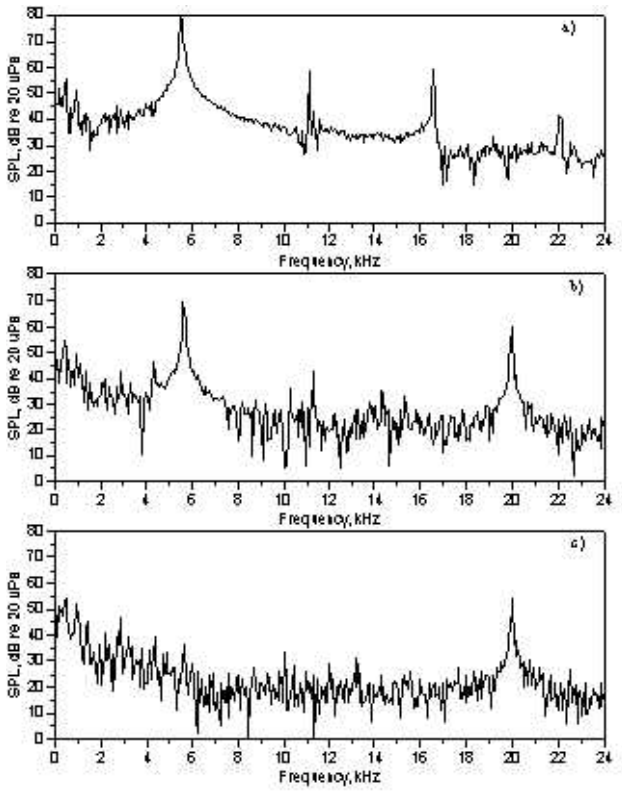

Figure 11 Sound Pressure Spectrum (a) before control activation, (b) during partial control, (c) after synchronization [1]

If dither control is applied to the brake prior to the establishment of squeal, then the squeal is prevented from occurring. Figure 12 presents the sound pressure level spectrum as a function of time as the braking conditions are varied. The brake system was brought into braking conditions that normally produce squeal, after a few seconds control was turned off and then on again. In the plot there is a strong response at the control frequency for the first four seconds until control is turned off. There are no other prominent (>60 db) responses during this time. When control is removed a new response appears at the squeal frequency of 5.7 khz. This response remains until control is turned back on at which time the 5.7 khz squeal response is suppressed and the 16.8 kHz dither frequency response returns. This plot clearly demonstrates dither control's ability to prevent and suppress squeal.

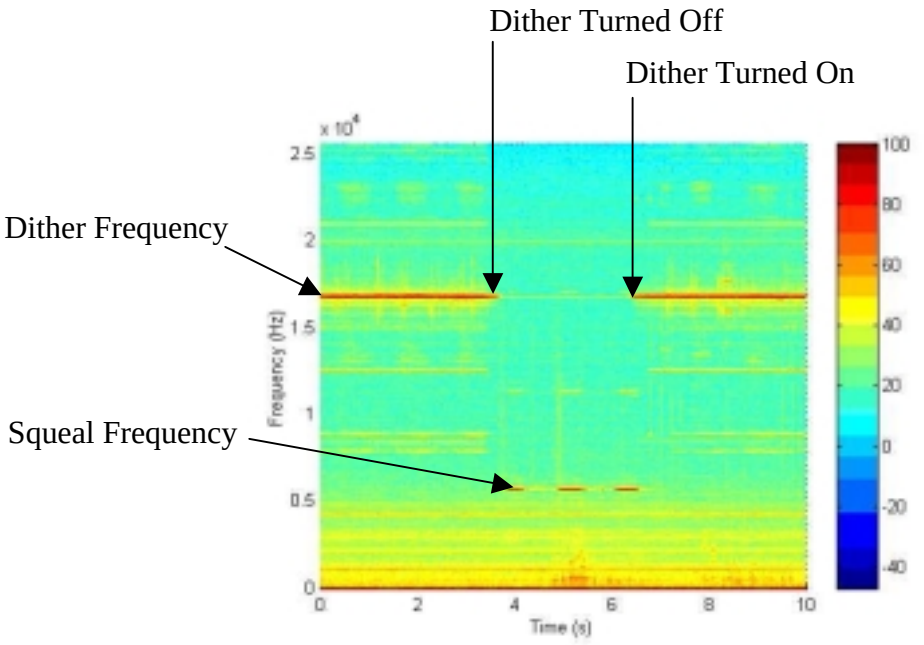

Figure 12 Waterfall Plot Illustrating the Prevention and Elimination of Brake Squeal Using a 16.8 kHz Control Signal [1]

1.5 Motivation

Clearly brake squeal is a problem for the automotive industry. Dither control has been shown to suppress and prevent brake squeal from occurring but this control's impact on braking effectiveness has not been established. For normal dither control to be useful to the automotive industry the control implementation needs not interfere with normal braking operations. It was the purpose of this research to experimentally establish the impact of normal dither control on the system's braking torque.

CHAPTER 2

BRAKE DYNAMOMETER AND DATA ACQUISITION SYSTEM

This chapter presents experimental hardware and software used to investigate the effect of dither control on the effective braking torque for an automotive braking system under light to moderate braking conditions and low rotor speed. The experimental setup used is a modified version of the test rig discussed in detail in [1, 16, 17]. This section provides an overview of the entire apparatus and a detailed explanation of all new or modified components.

2.1 Brake Dynamometer

Floating caliper disc brakes were installed on a brake dynamometer, depicted schematically in Figure 13. A General Electric 40 horsepower constant speed motor drives the system. To simulate low vehicle speeds a 24.1:1 gear reducer was installed between the motor and the rotor. A torque sensor was installed between the output of the motor and the gear reducer. This location was chosen to better utilize the measurement range of the sensor. The rotor is connected to an automotive half shaft, which is connected to the output of the speed reducer via a flange connection. The brakes are a standard floating caliper brake assembly as discussed earlier. The brake pressure is applied using a master cylinder, which is operated using a linear actuator.

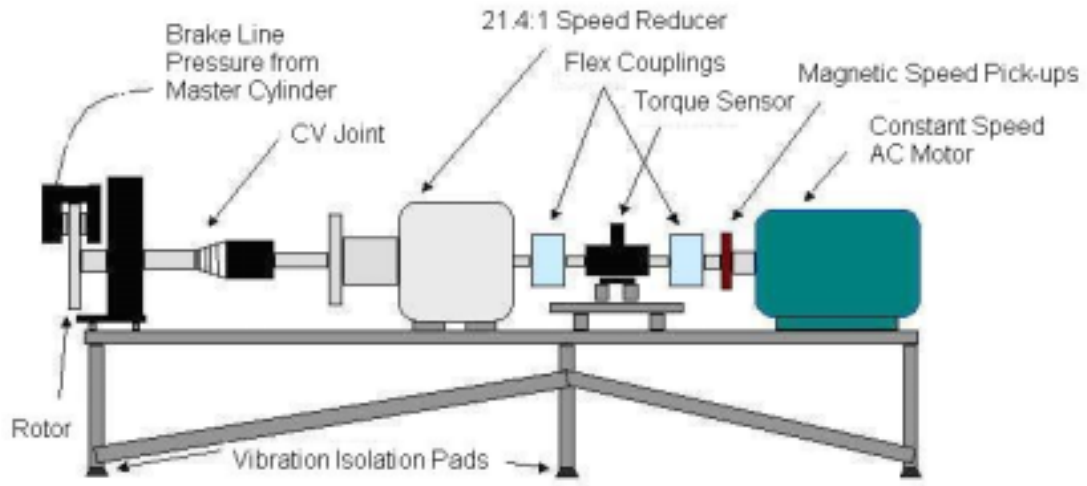

Figure 13 Brake Dynamometer

2.2 Controls

A constant brake pressure and rotor speed is necessary to obtain a stable and repeatable measure of the braking torque. The motor is controlled by a Parajust speed controller, which is operated manually and is not tied into the system's other controls. Figure 14 shows the arrangement of a linear actuator used to control the position of the brake master cylinder. Sending digital pulses to a servo motor controls the position of the actuator. Therefore the control program needs to supply the actuator with a direction and speed for each pulse. The control software used in this application was Labview. The brake pressure was controlled using a proportional, integral, derivative (PID) controller. The brake line pressure is measured with a pressure transducer and compared to the requested brake pressure to produce the error signal for the PID controller to minimize. The gains for the controller were found using a trial and error approach to find a combination that provided the most constant and stable brake pressure.

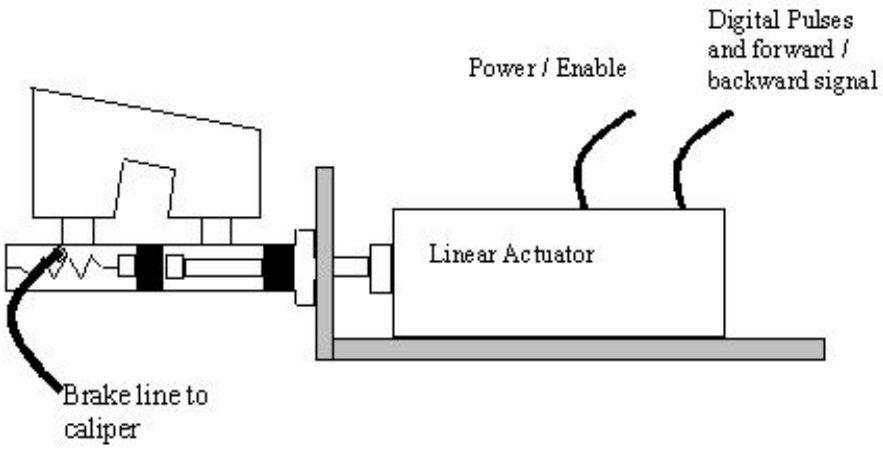

Figure 14 Linear Actuator [1]

2.3 Dither Implementation System

The dither signal was introduced into the braking system in the normal direction using an actuator located inside the brake piston as shown in Figure 15. The dither actuator consists of a piezoceramic (PZT) stack, load cell and housing. The dither actuator has one end in contact with the brake piston and the other end in contact with the inboard brake pad.

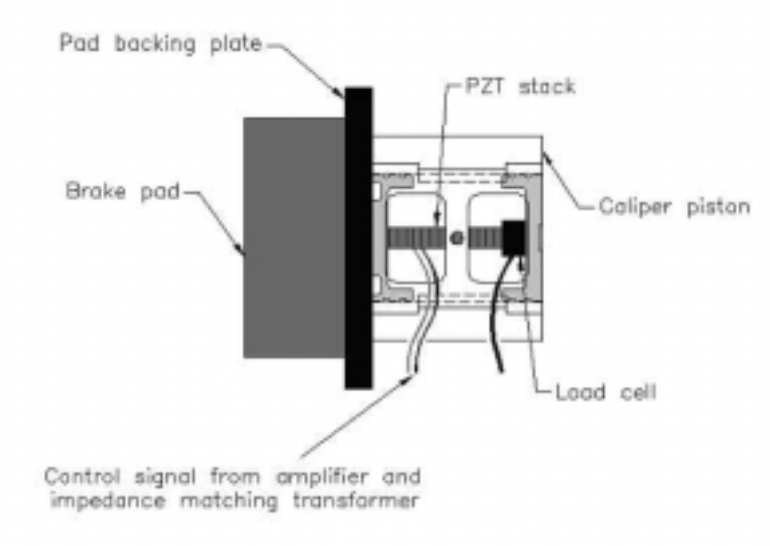

Figure 15 Piezoceramic Actuator

This research used a pre-loaded dither actuator design. Figure 16 shows an assembly drawing of this device. The PZT stack is housed in a steel cage using spherical bearings to keep it aligned vertically. A load cell is located between the stack and the closed end of the housing to measure the normal dither force. A spring washer is used to provide a pre-load onto the PZT stack. Assembling the actuator and installing shims between the load washer and the spring washer applies the pre-load. The number of shims used determines the preload provided. An arbor press is used to compress the spring washer while the snap ring is installed. This actuator design allows for different pre-loads, thereby changing the dynamic forces seen by the brake pads.

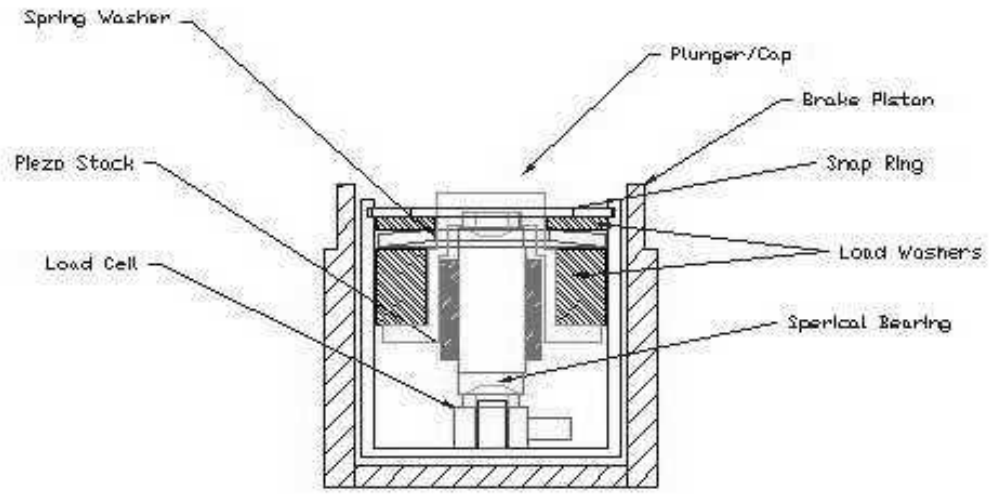

Figure 16 Pre-loaded Actuator Assembly

The PZT stack is driven by a control signal voltage applied across its terminal leads. Figure 17 show the string of power electronics used to generate this signal. A Hewlett Packard 33120A function generator generates the signal. This output is passed through a potentiometer with a 0-1 gain range and an on/off switch capability. The signal is then amplified by a Crown CE4000 audio amplifier, which has the capacity for 1200

watts per channel for a 4 ohm load and 2800 watts in bridge mono mode. For this application the amplifier was used in the bridge mono configuration. The amplified signal is sent to the Krohn-Hite MT-56 impedance matching transformer. The matching transformer is designed to supplement the output capabilities of the audio amplifier because the PZT stack is a capacitive load. The load voltage is monitored using a 100:1 attenuation probe and a Tektronics 2200 series oscilloscope. The PZT stack itself is a 900 nF device with 48 active layers.

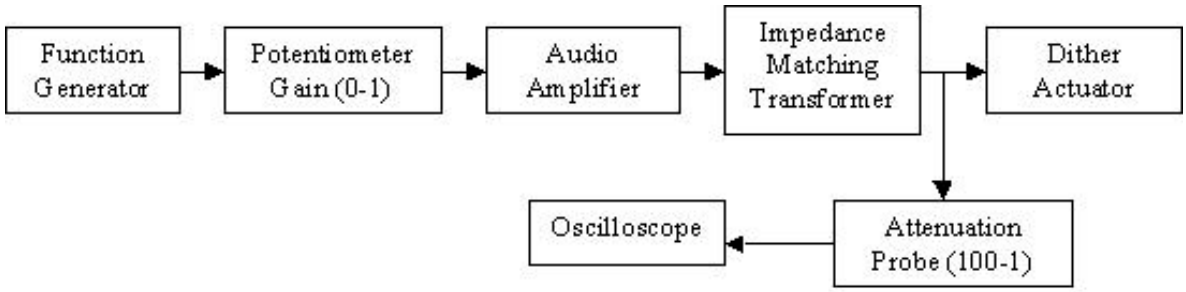

Figure 17 Drive Voltage Flow Chart

2.4 Transducers

Braking conditions are used to 'characterize' brake squeal and because brake squeal is a complicated phenomenon careful documentation of experimental parameters such as brake pressure, brake pad temperature, acoustic response and surface vibration is required. Squeal is associated with a set of brake pressure and rotor speeds where squeal is present. Brake squeal is a temperature dependent event with squeal diminishing as brake pad temperature increases. Several different squeals can exist at any specific set of braking conditions so the frequency of the squeal and the mode of vibration is frequently used to help distinguish squeals. The dither control signal is characterized by its

frequency, waveform type, duty cycle, voltage amplitude and normal force amplitude. Of course, to asses the impact of dither on braking effectiveness, the braking torque must be measured.

A Lebow model 1605-5K rotary transformer torque sensor was installed between the output of the motor and the input of the gear reducer to measure the braking torque of the system. The torque sensor generates a voltage signal proportional to the resistance change of its strain gage network. This change in resistance is proportional to the degree of deformation and in turn the torque on the structure. Figure 18 shows the Wheatstone Bridge configuration in which the strain gages are connected. This configuration acts as an adding and subtracting electrical network and allows compensation for temperature effects as well as cancellation of signals caused by extraneous loading. A fixed excitation voltage is applied between A and D of the bridge. A torque applied to the structure unbalances the bridge, causing an output voltage to appear between B and C. Since the shaft of the torque sensor is rotating, a rotary transformer is used to transfer the signal voltage from the rotational element to a stationery surface. A Daytronic 3278 signal conditioner supplies two output channels with a DC to 2 Hz and DC to 400 Hz passband filter, respectively. The instrument is calibrated to within 0.05% of full scale, which is 391.83 N-m. For this research that results is an uncertainty of +/- 0.196 N-m. The 2 Hz passband channel was used.

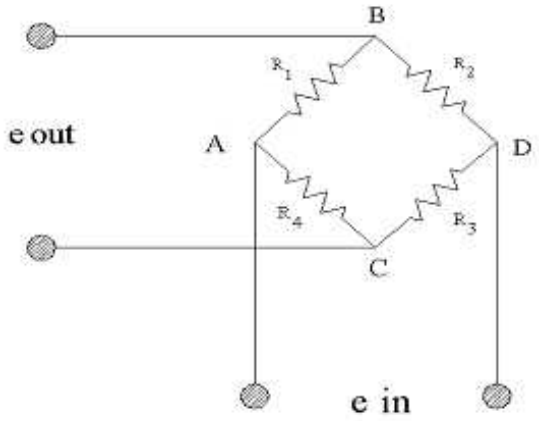

Figure 18 Wheatstone Bridge Strain Gage Network

A Kistler type 9011A quartz load washer was installed between the piezo-ceramic actuator and the brake piston, as shown in figures 15 and 16, to measure the normal dither force during squeal suppression. Quartz load washers are piezoelectric force transducers. A Kistler type 5010B dual mode amplifier is used as a charge amplifier. The load washer has an uncertainty of +/- 10 N.

A Sensotec model Super TJJE pressure transducer was used to measure the brake line pressure. This transducer is capable of measuring fluid pressure up to 6.89 MPa with an accuracy of +/- 0.05 percent which provides an uncertainty of +/- 0.003445 MPa. The pressure reading served as the feedback for the brake pressure PID controller.

The brake pad temperature was measured with a standard K-type thermocouple. A K-type thermocouple has an uncertainty of +/- 0.2 C with a maximum temperature capability of 871 degrees centigrade. A thermocouple was inserted into the in-board brake pad to monitor the brake pad temperature.

A Larson Davis model 2540 free field microphone was used to measure the acoustic response of the system during the different braking conditions. A Larson Davis

model 2200C power supply and Larson Davis model PRM900C preamplifier were used to condition the output signal.

A Polytec scanning head laser vibrometer, model OFV-055, was used to measure the surface velocity of the braking components. The primary advantage of using a scanning laser Dopper vibrometer (LDV) is that the measurements are non-contact, eliminating the added mass errors from accelerometers and the easier treatment of use with rotating objects. LDV's measure the Doppler shift of the laser light's frequency; furthermore, the magnitude of this shift is related to the normal velocity of the light-scattering, or vibrating object. The LDV detects the scattered beam that is phase modulated by the surface vibration, and the frequency difference between the reference and detected beams results in beats that are resolved into the time domain. Two types of LDV systems, single beam and dual beam, measure the out-of-plane and in-plane surface velocities, respectively. The OFV-055 is a single beam vibrometer and measures only vibration normal to the path of the beam.

2.6 Data Acquisition

The experimental test rig was designed for maximum flexibility in data acquisition capabilities. The normal dither force, actuator control voltage, acoustic pressure signal and rotor surface velocity require a sampling rate above 50 kHz but the brake pressure, brake pad temperature, and braking torque can be sampled at a much slower rate. Figure 19 shows the general configurations used in experimental testing. Two data acquisition computers and an oscilloscope were used to record or monitor all pertinent experimental quantities. The PC controlling the Polytec equipment has the capability to record the surface velocity data and one other data acquisition channel. This

channel has a maximum sampling capability of 512 kHz. A sampling rate of 128 kHz was used in this research. This channel was used to monitor the sound pressure during experimental testing or to record the normal dither force. The maximum dither frequency used is around 30 kHz and the acoustic response of the system is monitored up to this same range. A Labview virtual instrument (VI) was used to implement the PID controller discussed earlier and record brake pressure, brake pad temperature, and braking torque data. This data was collected using an NI4351 data acquisition card with a max sampling rate of 60 Hz. The torque on the motor side of the gear reducer was measured using the rotary transformer torque sensor. The longitudinal input force as well as the sound pressure were monitored but not recorded during these tests. The normal dither force was manually recorded for each experiment.

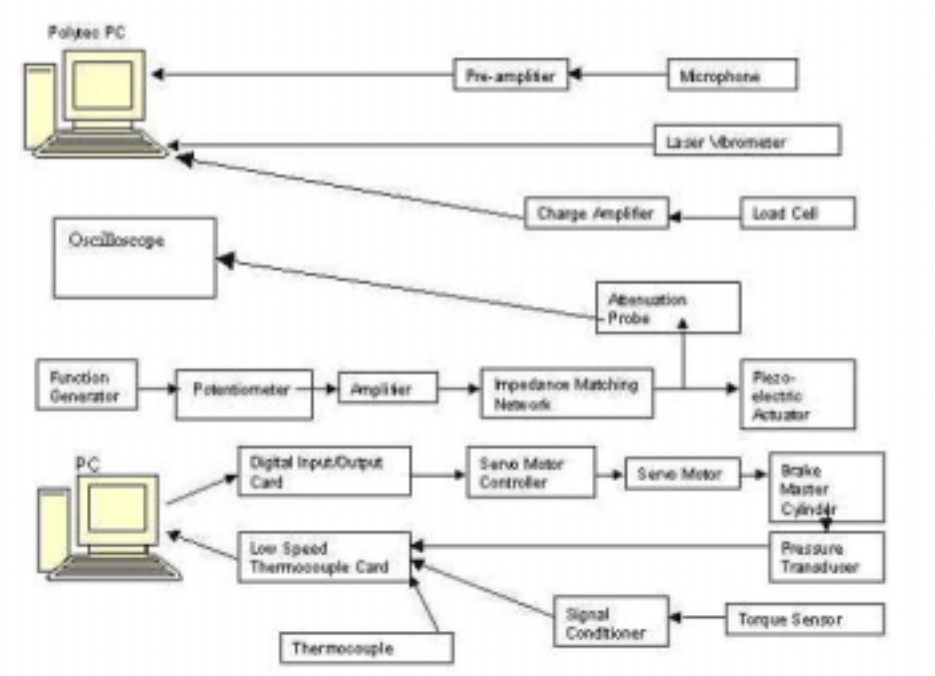

Figure 19 Data Acquisition System

CHAPTER 3

EXPERIMENTAL METHODOLOGY

This chapter presents the experimental methodology used to determine the effect of normal dither control on braking performance. To isolate the effect of dither on braking torque other parameters that could affect braking torque such as brake pad temperature and braking conditions needed to be removed from the experimental process. A statistical verification was also performed to ensure that the results were statistically significant.

3.1 Brake Squeal Characterization

In this research brake squeal is characterized by two major components: squeal frequency and the vibration pattern of the rotor. Squeal was found using a trial and error testing matrix. By continuously running the brake dynamometer at different combinations of brake pressure and rotor speed the system was worn in and squeal was found. The same brake squeal can be present for multiple sets of braking conditions. The frequency content, the fast fourier transform (FFT) of the acoustic response, of the squeal was recorded at the start of each test to monitor the evolution of the squeal response. The Polytec data acquisition channel was used with a sampling rate of 128 kHz and 30 averages. The scanning laser vibrometer was used to map the rotor's vibration response pattern (mode shape) to further distinguish between different brake squeals. Figure 20 shows the 79 scan points used to determine the vibration pattern. The braking system stopped producing brake squeal during the early phases of data collection so the focus of the research is on the torque impact of different dither signals.

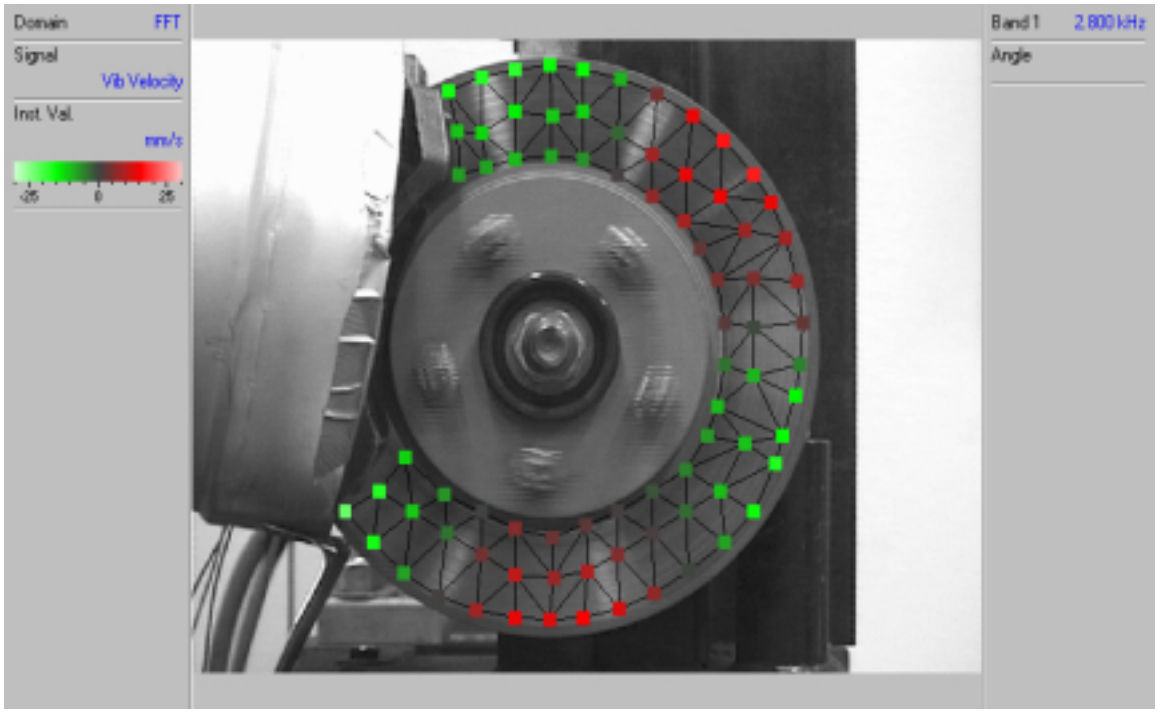

Figure 20 Scan Points used for Vibration Pattern Identification

3.2 Dither Control Signals

Dither control signals are classified by their frequency, force amplitude, waveform type and burst parameters. In this investigation only the frequency and amplitude of the signals is varied. An interesting trend that was discovered in Cunefare & Graf's work was that certain frequencies obtained 'control' of the system using significantly lower input voltages. These frequencies were values that produced the best excitation of the system for a given input. In order to choose dither control frequencies that were most likely to produce control, a transfer function between the dither actuator's voltage and the surface vibration of the brake rotor was measured. This was first done with a stationery rotor. This test was repeated for a variety of brake pressures to determine the effect of the boundary conditions on the system's response. To experimentally validate Hess & Soom's prediction that the maximum torque reduction

occurs at the primary resonances, this procedure was repeated during regular braking conditions as well [9].

Transfer functions between the load voltage and rotor response were produced to determine dither signal frequencies which result in the most system response for a given input voltage. These transfer functions were produced using a Siglab two channel data acquisition system. Channel one was configured to read the load voltage from the attenuation probe and channel two was the output of the laser vibrometer. Several points on the rotor were used as response points. A swept sine signal was used as the input to the PZT. These tests were performed while the rotor was stationery to isolate the peaks in the static rotor response. This test was repeated for several different brake pressures to determine the boundary condition effect on the rotor responses.

Another useful tool is the dynamic transfer function between normal dither force and rotor response. This provides the natural frequencies of the system during a specific braking event. Peaks in this response were also used as dither control frequencies to test the conclusion from Hess & Soom [9] that the greatest reduction in braking torque occurs near primary resonances.

3.3 Torque Testing Procedure

This section describes the process of acquiring, tabulating and reporting of the experimental results. During each test the brake pad temperature, brake pressure and braking torque are recorded in two, 150 sample, data blocks. The normal dither force and PZT voltage were monitored using an oscilloscope during testing but a time history was not collected. The mean value of each data type (brake pressure, brake pad temperature and braking torque) were tabulated for each test case and recorded. This test is repeated

three times representing three different dither application cases. The first case is where the dither signal is not applied (temperature case, labeled as "Temp"), the second is when dither is applied during the first data block (test case 1, labeled as "T1") and third when dither is applied to the second data block (test case 2, labeled as "T2"). Brake pad temperature is included in data acquisition in this manner to ensure that each trial is completed over approximately the same temperature range. It was found that the system's braking torque was temperature dependent so it is important to ensure that each trial was conducted over the same range of temperatures. The change in brake pressure over the data blocks is monitored to ensure that the PID controller maintained a stable brake pressure throughout the test. If there is a statistically significant change in pressure it is removed from the torque results. A ten percent change in brake pressure results in a ten percent change in braking torque, given that the rotor speed is held constant. This allows the pressure dependence to be subtracted out of the torque results using

$$\text{Torque}_{\text{Final}}^{\%\text{Change}} = \text{Torque}_{\text{Raw Data}}^{\%\text{Change}} - \text{Pressure}_{\text{Raw Data}}^{\%\text{Change}}.$$

In order to isolate the effect of different parameters on the torque impact a reference dither signal is first analyzed. For this research the reference signal is a 25.6 kHz sine waveform signal, 125-volt PZT excitation, 200-Newton dither force amplitude applied under 0.6205 MPa of brake pressure with a motor speed of 1100 rpm. After the effect of this reference signal is established each parameter: dither frequency, dither force amplitude, brake pressure and motor speed, is varied one at a time to asses the affect of each separately.

3.4 Statistical Analysis

The percent change in torque and pressure values are only calculated when the mean values are deemed to have a statistically significant difference, as indicated from a t-test. A t-test determines if the mean value of two groups are statistically different from each other. The t-test is calculated using the mean, variance and number of samples for each group. The difference in means is scaled by the standard error of the difference. Taking the variance of each group and dividing it by the number of samples in that group, adding these two quantities and taking the square root, computes the scale factor. The formula for the t value is

$$t = \frac{\bar{X}_T - \bar{X}_C}{\sqrt{\frac{var_T}{n_T} - \frac{var_c}{n_c}}} \cdot$$

This t-value is used with a table of percentiles of t distribution to test whether the ratio is large enough to say that the difference between the groups is not likely to have been a chance finding.

This experiment was constructed to determine if the means of two samples were statistically different from one another. First, the size of the data block taken needed to be determined. The trade off associated with block size was lowering the variance of the mean of the data block versus the time it takes to collect that many data points. With constant brake pressure applied, the more data points taken, the higher temperature the brake pads would reach. A balance of these two factors leads to a block size of 150 points. This range kept the brake pads under 50 C and provided a 95.0% confidence interval on the order of 0.3% of the mean value. A t-test was used to determine if the mean values were statistically significantly different. The t-test returns a P-value, which

is the likelihood that the t-test results are not valid. For instance, a P-value of 0.05 means that the means of the two samples are statistically different 95.0 % of the time. The t-test assumes the data from each sample has equal variances. An F-test is run on this data to confirm that the data does indeed belong to samples with equal variances. The F-test assumes that the data is from a normally distributed population. Using the standardized skewness and standardized kurtosis numbers the population can be tested as normally distributed. Each experiment was subjected to these groups of statistical tests to ensure that the populations were normally distributed with equal variances.

The mean values obtained in each trial were then used to calculate a 'mean of means' value that determines the overall results of each test. The mean value data is used as the new data population and the statistical analysis is repeated. This provides a single number to quantify the effect of each test case. The number of trials for each test case is based upon two parameters that are monitored during testing, the P-value relating the mean of means and the percent difference of these torque values. For each test case, trials are repeated until the P-value converges either indicating a statistically significant difference between the means (converging below 0.05 for 95.0 % confidence) or indicating the means are not different (converging above 0.05). When the P-value converges below 0.05 another criterion must be met, that is, the percent difference between the two mean values must also converge. This procedure ensures that the test clearly indicates whether there is a statistically significant difference and clearly defines what that difference is.

CHAPTER 4

RESULTS

This chapter presents the results of the experiments to determine the effect of dither control on braking torque. These experiments show that normal dither signals have little to no effect on the system's braking torque. This result is very encouraging to the further development of dither control technology. The following sections of this chapter discuss the results of brake squeal characterization, dither implementation system transfer function tests, reference dither signal effect, effect of braking conditions and the effect of changing dither parameters.

4.1 Brake Squeal Characterization

Brake squeal is a difficult event to produce and reproduce. It is difficult to find a set of braking conditions that produce brake squeal and there are no guarantees that brakes that do squeal will do so every time these conditions are repeated. This makes characterizing brake squeal a very important tool. Characterizing brake squeal by the frequency spectrum of its acoustic response and the corresponding vibration pattern of the rotor provides a method of tracking system changes. Table 2 shows the braking conditions and peak acoustic response levels associated with a repeatable squeal found with this braking system. The reference braking conditions used were a brake pressure of 0.6205 MPa and a motor speed of 1100 rpm, which translates to a vehicle speed of approximately 2.75 mph. These conditions produced the most consistent, repeatable and audible response.

Table 2 Brake Squeal Content

Brake Pressure (MPa)	Frequency (kHz)	L_p (db)	Frequency (kHz)	L_p (db)	Frequency (kHz)	L_p (db)
0.4826	2.680	81.2	4.477	72.3	8.961	51.6
0.5516	2.750	78.4	4.508	75.8	8.258	59.5
0.6205	2.758	89.1	5.516	70.1	8.281	64.1
0.6895	2.773	94.3	5.547	66.7	8.320	62.1
0.7584	2.797	97.0	5.602	71.1	8.391	60.5
0.8274	2.828	99.2	5.648	69.2	8.477	56.8
0.8963	2.852	91.9	5.711	62.5	8.563	55.3
0.9653	2.875	74.8	5.758	51.9	gone	-

Brake squeal at an individual set of braking conditions is characterized by its acoustic response and the vibration pattern of the rotor. Figure 21 shows the sound pressure level of acoustic response of the system in decibels (dB). Sound pressure level is calculated from the measured sound pressure in pascals (Pa) using $L_p = 10\log(P_{rms}^2/P_{ref}^2)$ with 20 micropascals as the reference pressure. Peaks in the response are located at 2.852 kHz, 5.703 kHz and 8.5 kHz. The response has the largest amplitude at the primary squeal frequency, 2.852 kHz. Figure 22 shows the vibration of the rotor at 2.852 kHz. This particular squeal appears to set the rotor into a (0,3) circumferential mode of vibration. Figure 23 shows the vibration of the rotor at 5.703 kHz and Figure 24 shows the vibration of the rotor at 8.5 kHz. These mode shapes are useful to aid in determining which system responses are contributing to the audible squeal response.

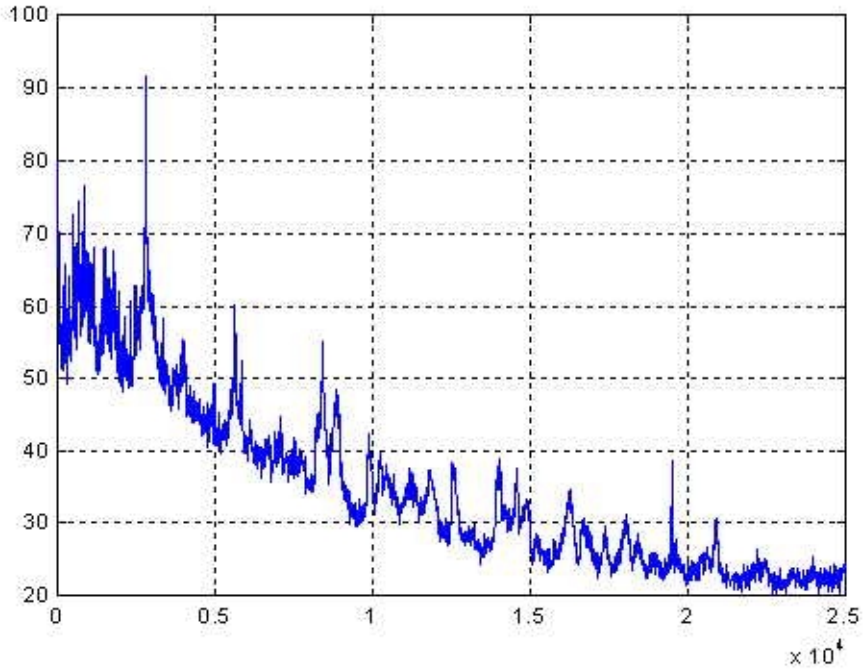

Figure 21 Acoustic Response of System Sound Pressure Level (dB) versus Frequency (Hz)

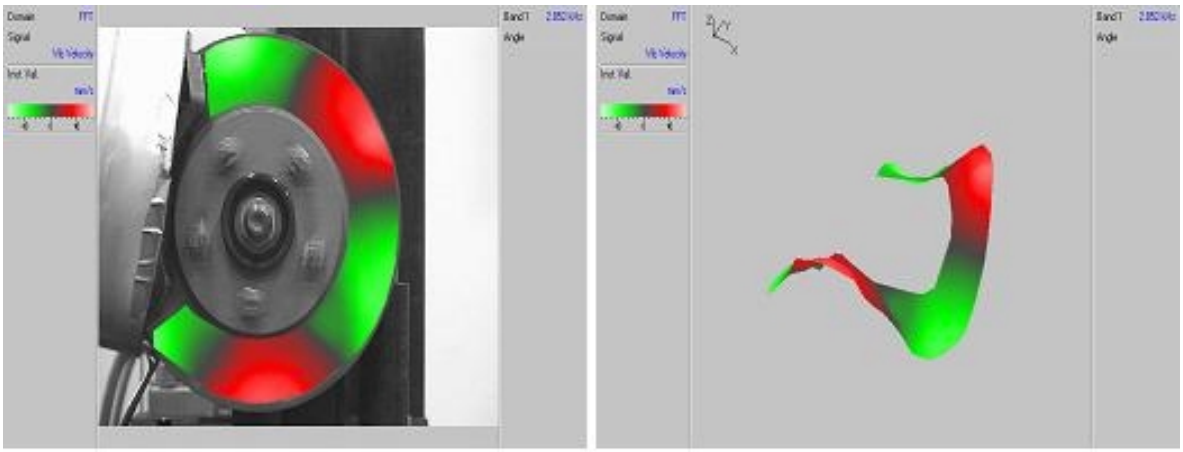

Figure 22 Vibration Pattern of Rotor During 2.852 kHz Squeal

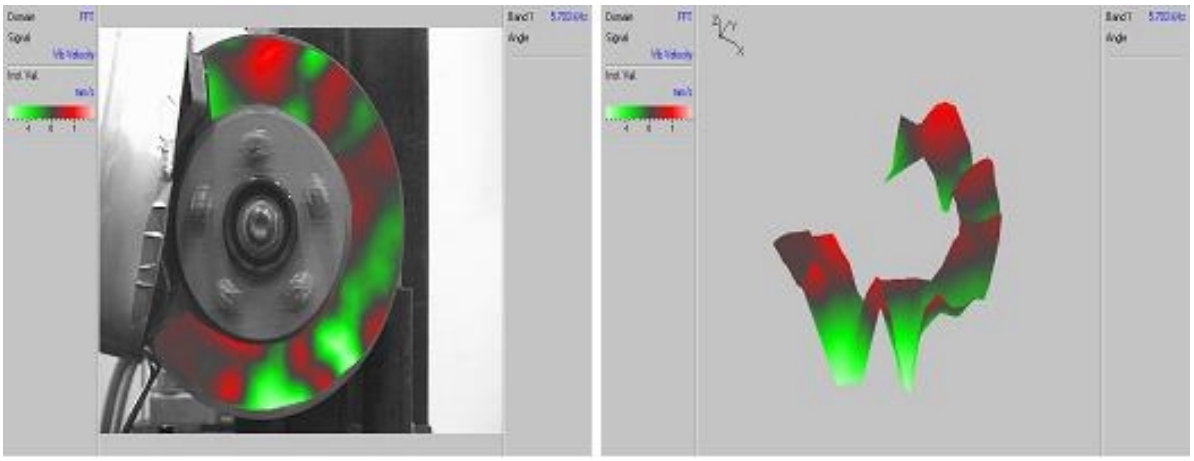

Figure 23 Vibration Pattern of Rotor During 5.703 kHz Squeal

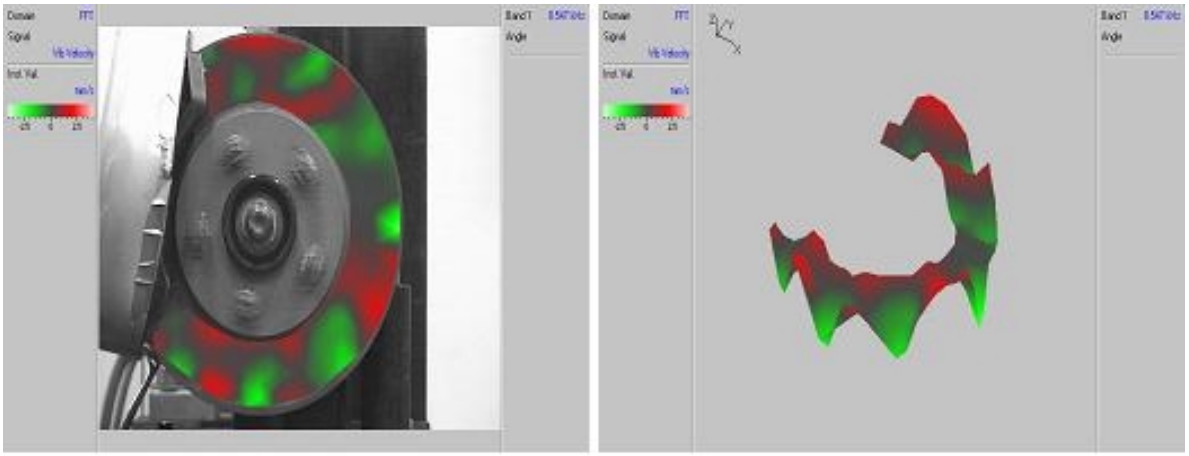

Figure 24 Vibration Pattern of Rotor During 8.547 kHz Squeal

Another interesting characteristic of brake squeal is to look at the amplitude of the rotor response while the system is squealing and when it is not. Figure 26 shows the FFT of the rotor response at a single point during braking conditions that cause squeal and the rotor response while the system is not squealing. Clearly this plot shows that the rotor does not vibrate significantly when the system is not squealing and has significant vibration at the squeal frequency when the braking conditions are changed to produce squeal.

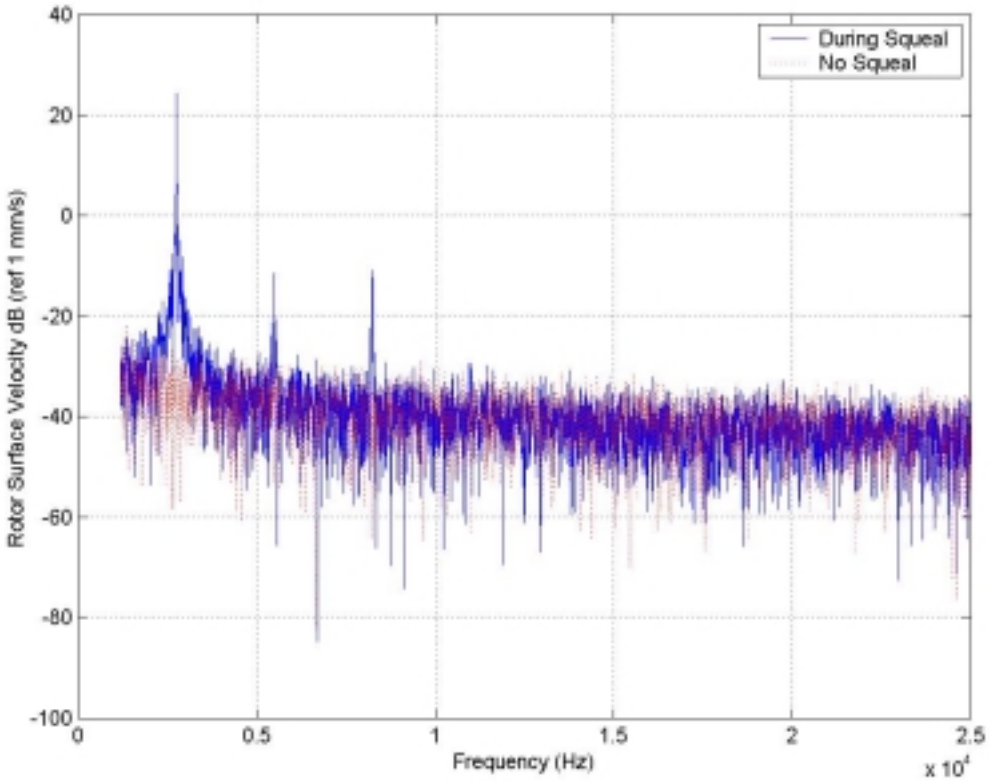

Figure 25 Brake Rotor Response With and With-out Squeal

In lieu of brake suppression tests, a procedure to choose dither control signals to maximize the likelihood of suppression was used. This particular brake squeal was only present for the first few weeks of testing so suppression results were not obtained. Figure 26 shows the rotor mode of vibration for the 5.7 khz squeal suppressed by Cunefare & Graf in previous research at Georgia Tech [1]. By comparing Figure 26 to Figure 23 it is clear that the squeal currently present in the system is not the same as what was analyzed previously. This result prevents us from assuming that the same dither control signals chosen by Cunefare & Graf would also suppress the current squeal. An interesting trend that was discovered in Cunefare & Graf's work was that certain frequencies obtained 'control' of the system using significantly lower input voltages. These frequencies were

values that produced the best excitation of the system for a given input. In order to choose dither control frequencies that were most likely to produce control, a transfer function between the dither actuator's voltage and the surface vibration of the brake rotor was conducted.

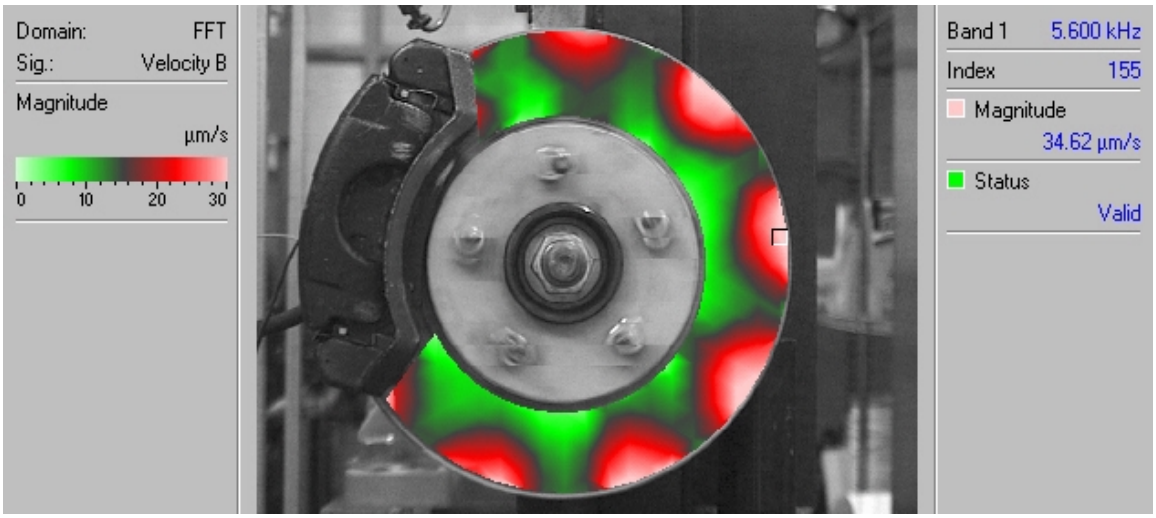

Figure 26 Vibration Pattern of Rotor During 5.7 kHz Squeal [1]

4.2 Transfer Function Tests

The static and dynamic frequency response of the rotor was obtained using the dither actuator as the input. Figure 27 shows the positions on the rotor where the transfer function was measured. The vibration pattern of the rotor was measured for each peak in static and dynamic transfer functions to establish a relationship to the squealing brake mode shapes.

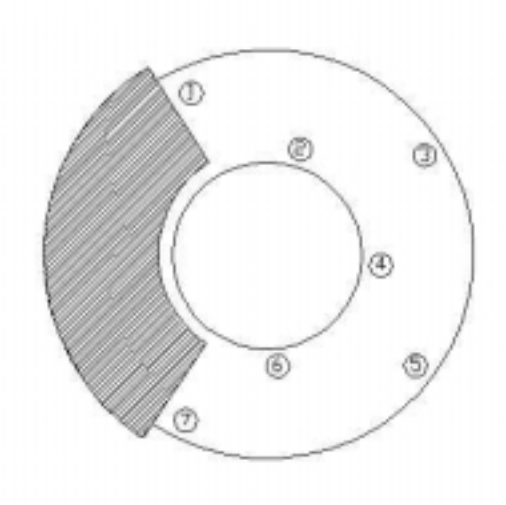

Figure 27 Data Acquisition Locations for Transfer Function Tests

Figure 28 shows the static transfer function over the frequency range of 1khz – 26 kHz. In the frequency range containing squeal there are prominent peaks at 2950, 4675, 6300 and 8100 Hz. It was shown earlier that the prominent peaks in the squeal response occurred at 2852, 5703 and 8547 Hz. Figures 29-32 show the rotor response to excitation at these peak response locations. The 2.852 kHz squeal and 2.950 kHz stationery response share a similar pattern of motion. The other squeal responses appear to be combinations of several rotor stationery modes. These results would tend to indicate that the squeal frequencies are related to rotor resonances, but not all rotor resonances result in audible squeal.

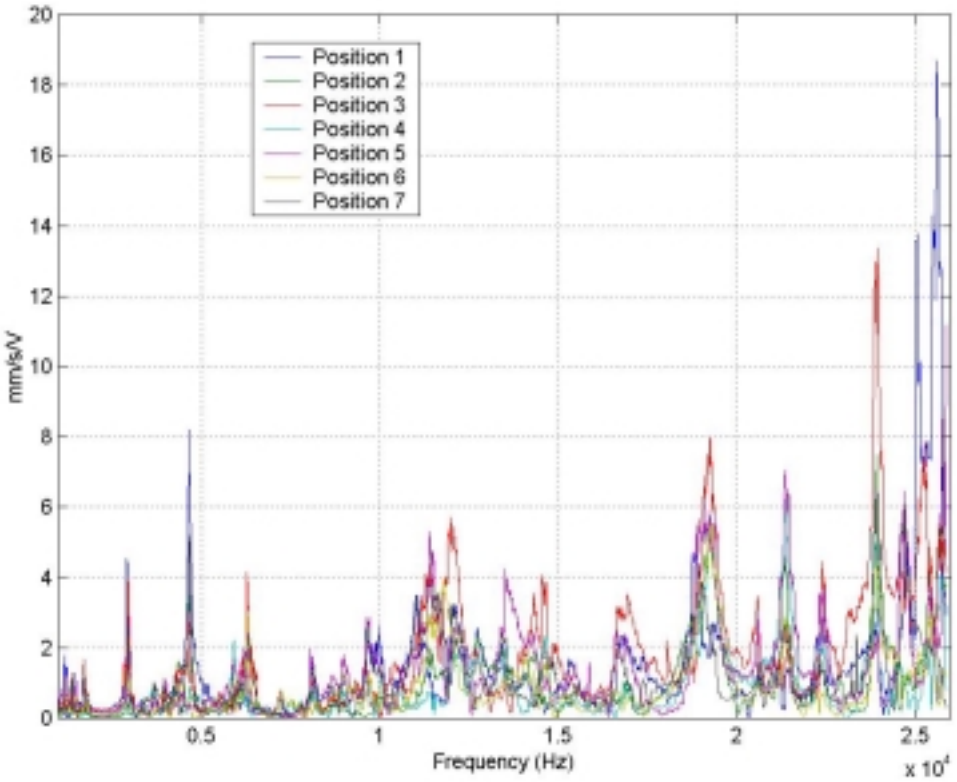

Figure 28 Rotor Transfer Function 1 kHz - 26 kHz

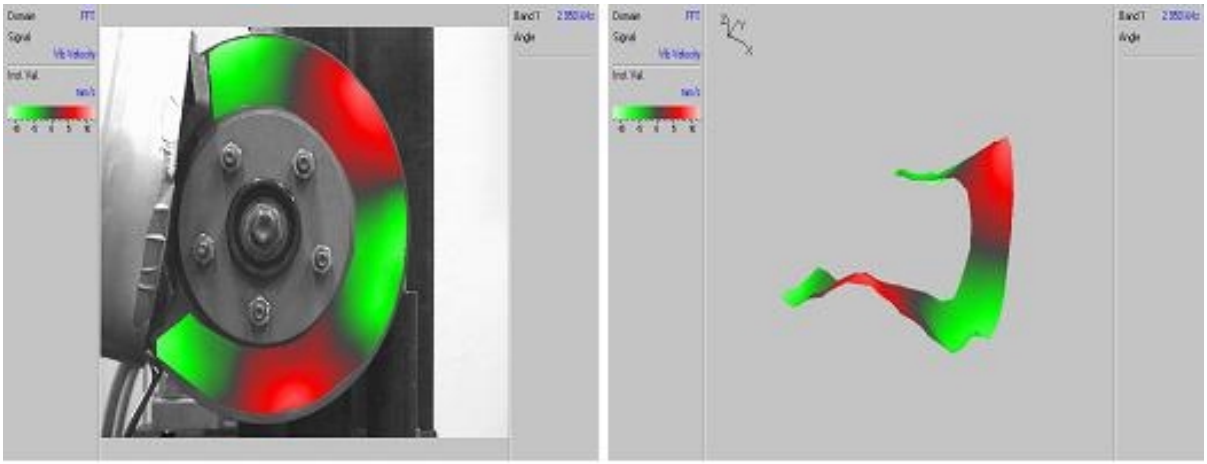

Figure 29 Stationary Rotor Response at 2950 Hz

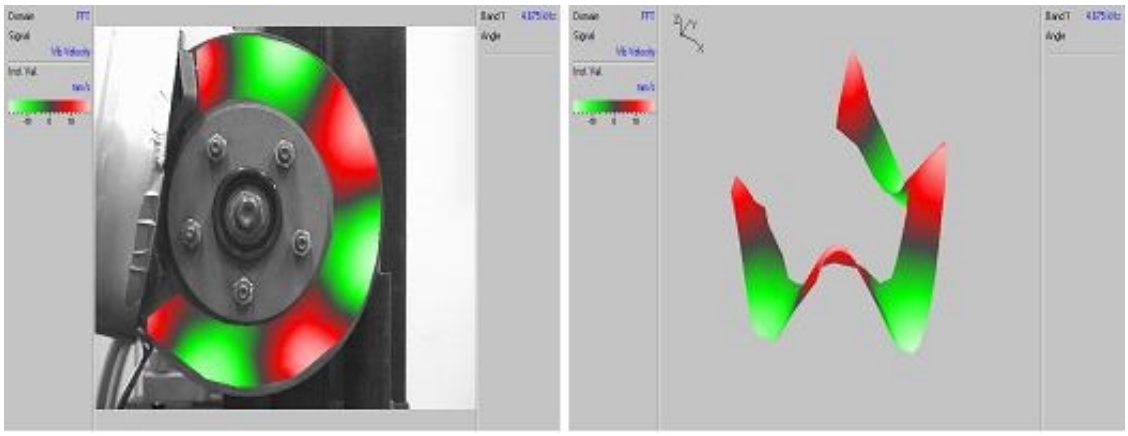

Figure 30 Stationary Rotor Response at 4675 Hz

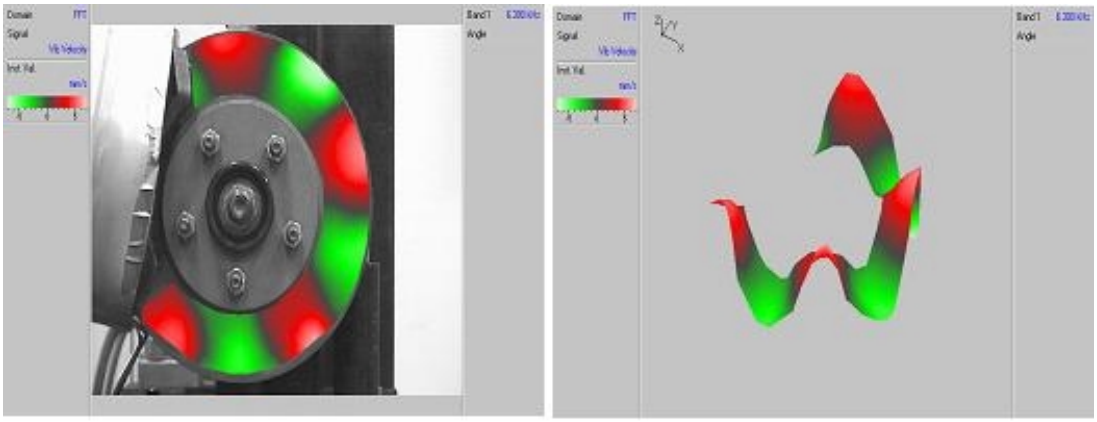

Figure 31 Stationary Rotor Response at 6300 Hz

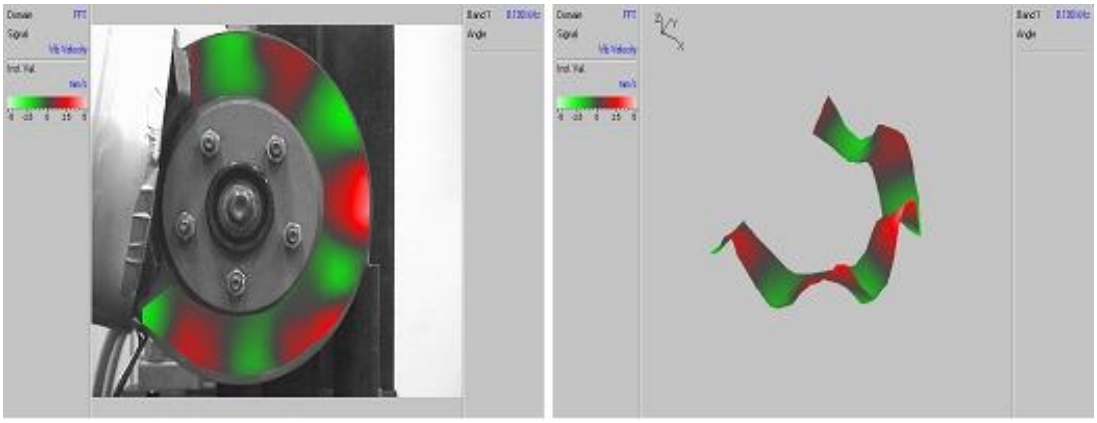

Figure 32 Stationary Rotor Response at 8100 Hz

The dither control frequencies chosen for this research were 4662.5, 6300, 12,000, 19,250 and 25,600 Hz. These frequencies all correspond to peaks in the rotor response tests.

All of the transfer function testing discussed so far was conducted at a brake pressure of 0.6205 MPa, but an interesting question is whether the rotor resonances change as the applied brake pressure changes. To establish this relationship the transfer function tests were repeated at position one for a wide range of brake pressures. Figure 33 shows a waterfall plot of the results of this test. Figure 33 shows that the peaks do not seem to shift in frequency but the amplitude of the response seems to have some pressure dependency. Figure 34 more clearly demonstrates the behavior of the 2900 Hz response. It is a contour plot of these transfer function tests centered around 2900 Hz. It clearly shows the peak response in this region shifting frequency as well as amplitude. This leads to the conclusion that this brake squeal is slightly dependent on changes in boundary conditions.

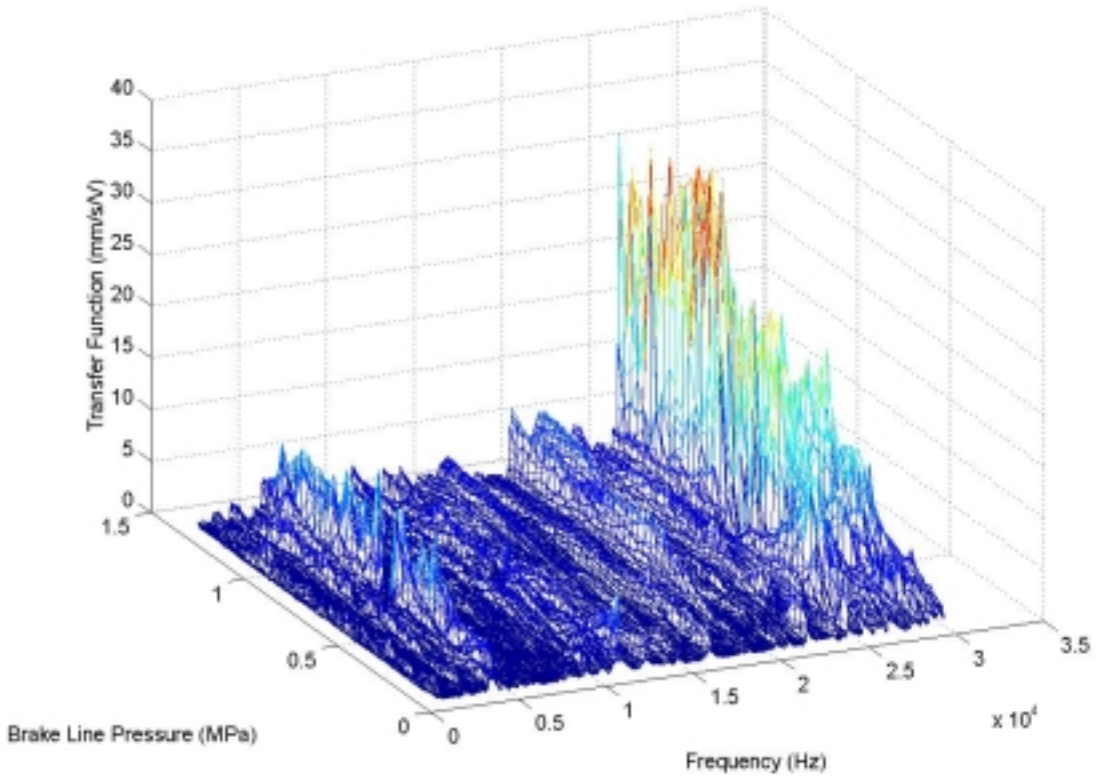

Figure 33 Rotor Transfer Function as a Function of Brake Line Pressure

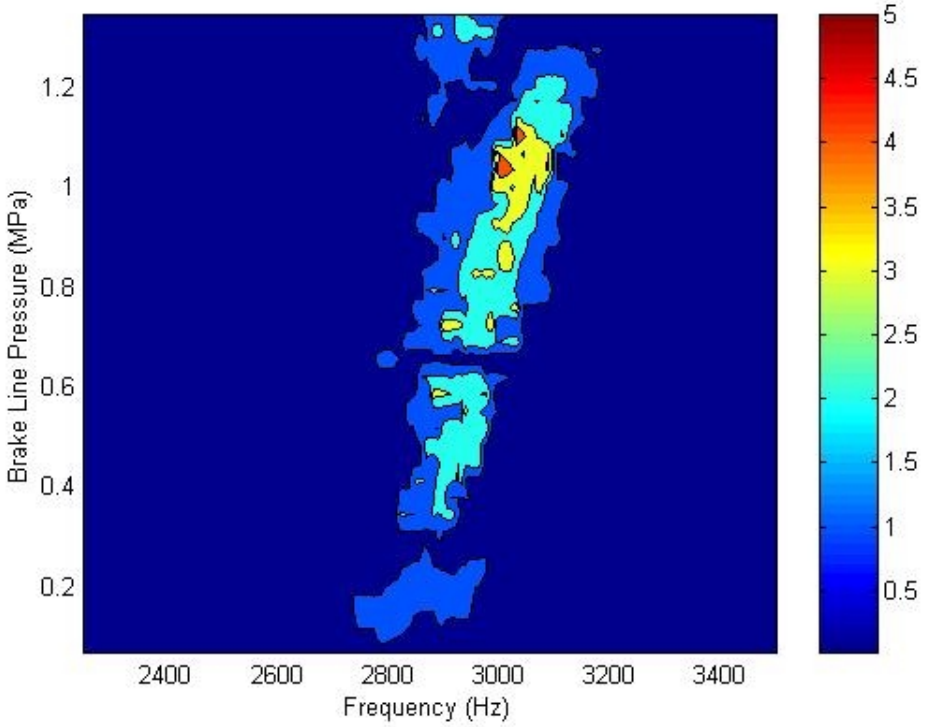

Figure 34 Rotor Transfer Function as a Function of Brake Pressure Centered Around 2900 Hz Response

The dynamic transfer function between normal dither force and rotor response was acquired using the same procedure as the static tests at a brake pressure of 0.6205 MPa and motor speed of 1100rpm. Figure 35 shows the dynamic transfer function. Hess & Soom predicted a higher level of reduction of friction force at frequencies near the system's primary resonance [9]. To test this theory dither control frequencies were chosen at peaks in the dynamic transfer function. The frequencies chosen were: 2.9, 4.5, 11.3, 18.66 and 24.5 khz. Figure 36 - 40 show the rotor response for the dither frequencies chosen from this response. These mode shapes lead to the conclusion that the dynamic interaction causes similar frequencies to have a higher number of node patterns and adds a circumferential dependence to the vibration pattern. Table 3 lists the

peaks in the squeal response, static transfer function and dynamic transfer function along with a description of the pattern of vibration. The major difference in mode shapes for the dynamic transfer function tests is the addition of a circumferential node. In all cases the mode shapes for the transfer function tests have much 'cleaner' shapes than that of the squeal response.

Table 3 Vibration Pattern Comparison

Squeal Response		**Static Transfer Function**		**Dynamic Transfer Function**	
Freq (kHz)	Description	Freq (kHz)	Description	Freq (kHz)	Description
2.852	6 nodes with no circumferential dependence	2.950	6 nodes with no circumferential dependence	2.900	12 nodes with added circumferential node
5.703	8 nodes with no circumferential dependence	4.675	8 nodes with no circumferential dependence	4.500	14 nodes with added circumferential node
8.547	10 nodes with no circumferential dependence	6.300	10 nodes with no circumferential dependence	11.300	Hard to distinguish pattern
		8.100	12-14 nodes with no circumferential dependence	18.660	Hard to distinguish pattern
				24.500	Hard to distinguish pattern

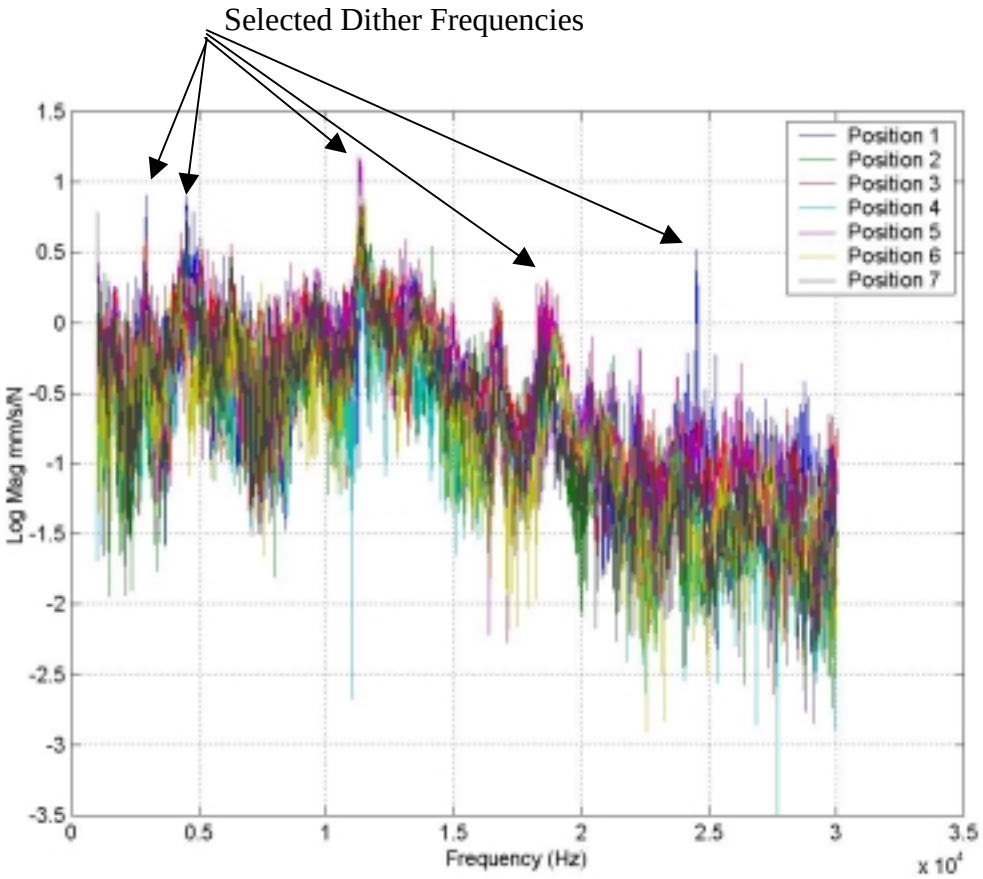

Figure 35 Dynamic Transfer Function, Selected Dither Frequencies: 2.9, 4.5, 11.3, 18.66 and 24.5 kHz

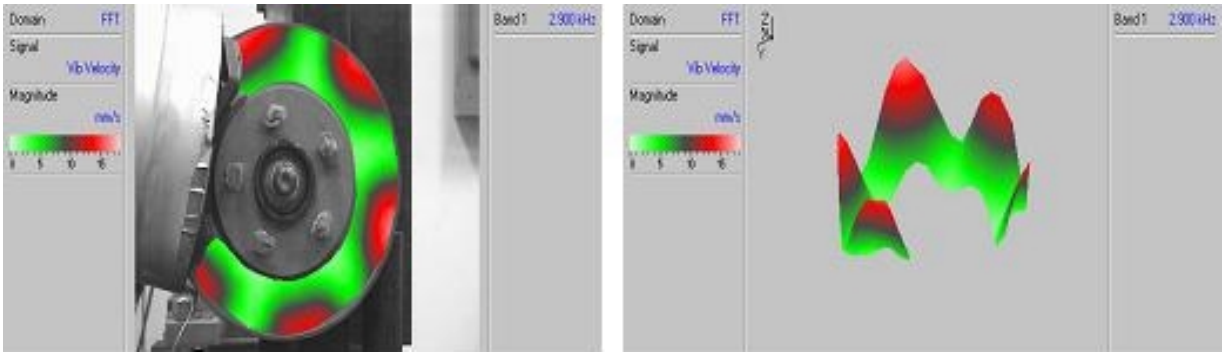

Figure 36 Dynamic Rotor Response 2.9 kHz

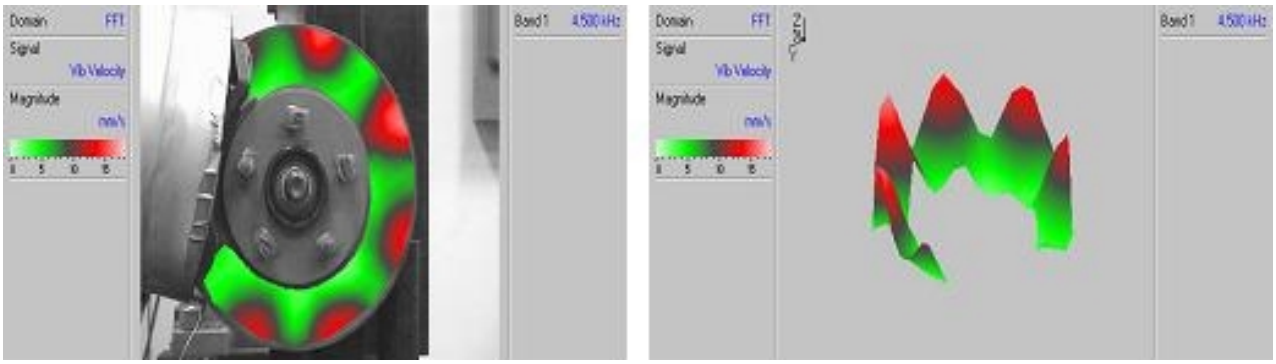

Figure 37 Dynamic Rotor Response 4.5 kHz

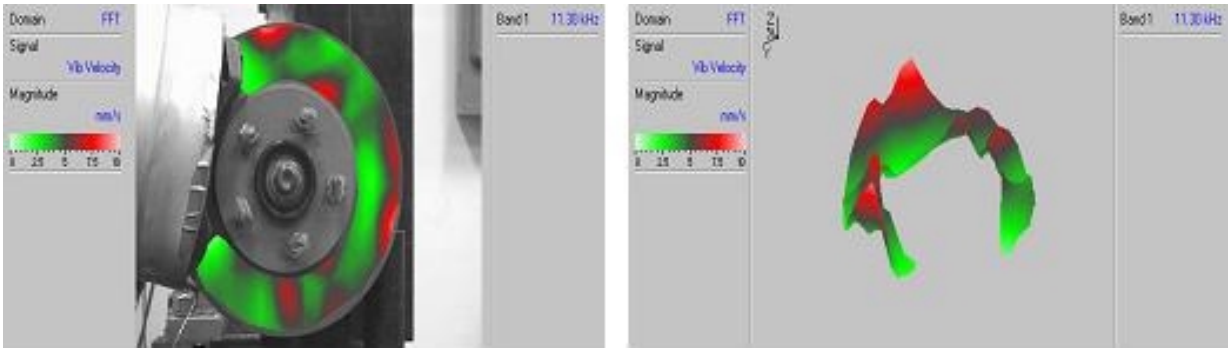

Figure 38 Dynamic Rotor Response 11.3 kHz

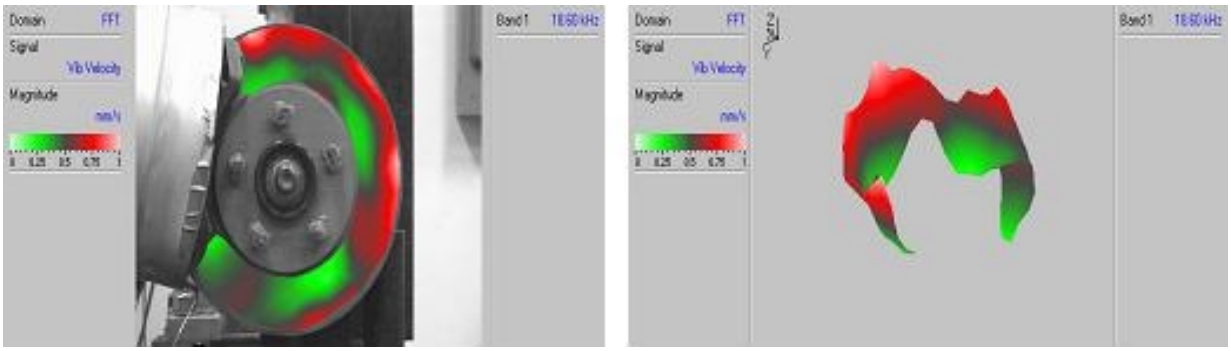

Figure 39 Dynamic Rotor Response 18.66 kHz

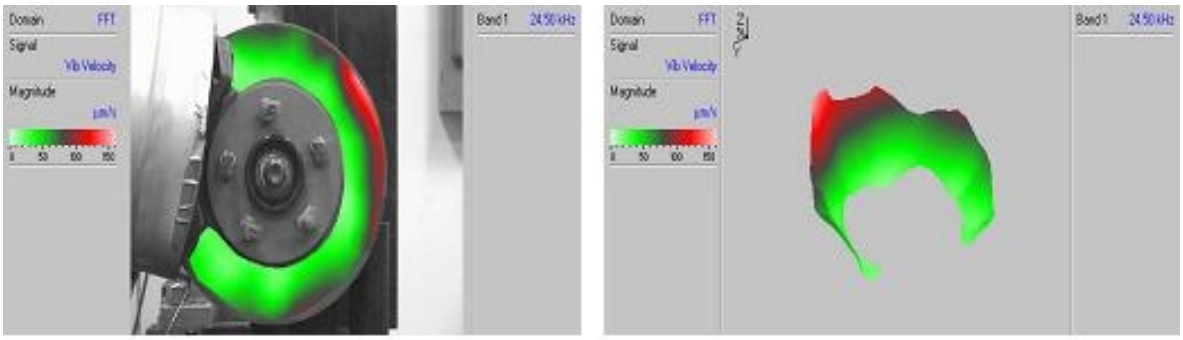

Figure 40 Dynamic Rotor Response 24.5 kHz

4.3 Reference Dither Signal Results

The reference dither signal was a 25.6 kHz sine waveform signal, 125-volt PZT excitation, 200-newton dither force amplitude applied under 0.6205 MPa of brake pressure with a motor speed of 1100 rpm (45.64 rpm rotor speed). Figure 41 shows the percent difference in braking torque as a function of the number of trials completed. Each point on the graph is a running average of all trials completed up to that point. For all three test cases the braking torque increased by between 5 and 8 percent between the two data blocks.

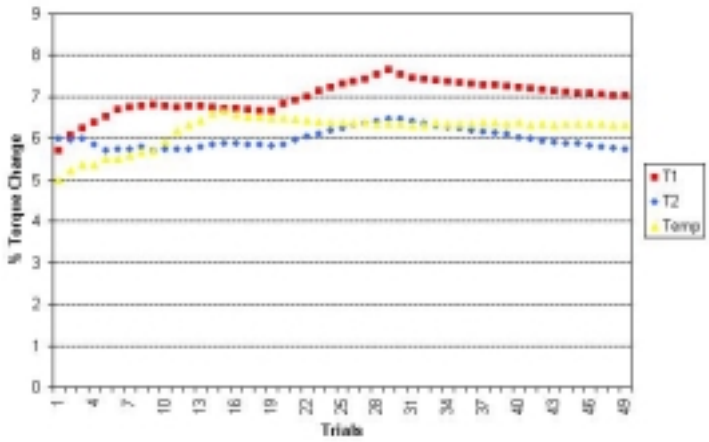

Figure 41 Percent Change in Brake Torque

To determine the specific effect of dither on the braking torque all other parameters must be removed from the results. For most trials the brake pressure is held within half of a percent of the mean value over the two data acquisition blocks. Figure 42 shows the percent difference in brake pressure using a running average as before. The T1 test has a fairly constant 0.2 percent change in pressure over the blocks while both other cases are very stable. The pressure variation is small but is removed from the torque results to ensure the most accurate portrayal of dither's effect.

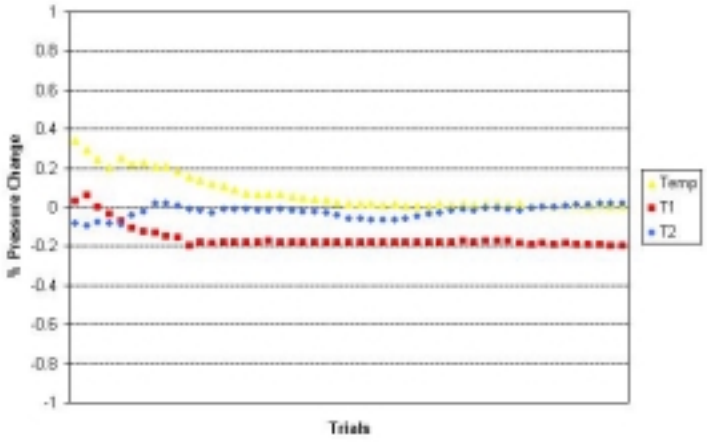

Figure 42 Percent Change in Brake Pressure

To isolate the effect of the dither signal from all other influences during the tests the temperature trials results are removed from the T1 and T2 tests. This is accomplished using the following formulas:

$$Torque_{1Final} = Temp_{pressure\ adjusted} - T1_{pressure\ adjusted}$$

$$Torque_{2final} = T2_{pressure\ adjusted} - Temp_{pressure\ adjusted}$$

Figure 43 is the running average plot for the T1 and T2 torque dependence after removing external effects in this manner. In this case the reference dither signal results in a torque change of -0.88 % and -0.64 % in each test case respectively. All other test cases are analyzed using this procedure and underlying torque reduction are compared

using these two numbers. In most tests the T1 and T2 torque difference numbers converge as these two values in figure 43. In all future discussions the torque results are presented as a range between these values.

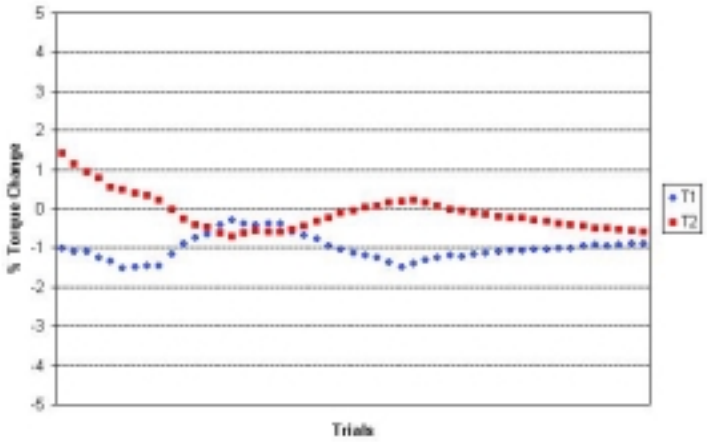

Figure 43 Final Torque Dependence

4.4 Effect of Braking Conditions

In practical application, dither control is not limited to one specific set of braking conditions; therefore it is of interest to determine the effect of braking conditions on the dither signal's effect. The reference dither signal is used with three brake pressure and three motor speed combinations. Table 4 displays the results from these tests. In each case the dither signal produces a small reduction in the average braking torque. Neither rotor speed or brake line pressure seems to dramatically affect the torque output of these tests.

Table 4 Torque Reduction Values for Variable Braking Conditions

Brake Pressure (MPa)	Motor Speed (rpm)	Vehicle Speed (mph)	Torque Impact
0.2068	1100	3.5	-0.88 to -0.65 %
0.6205	1100	3.5	-0.89 to -0.61 %
1.0342	1100	3.5	-0.55 to 0.38 %
0.6205	1000	3.2	-1.07 to -2.70 %
0.6205	1100	3.5	-0.89 to -0.61 %
0.6205	1200	3.8	-0.13 to -1.02 %

4.5 Effect of Dither Normal Force Amplitude

The reference dither signal was shown to have a small impact on the braking torque, now the effect of normal dither force amplitude is investigated. Dither control effectively suppresses and prevents brake squeal only after a threshold amplitude is reached [1]. To determine the effect of amplitude, the reference dither signal of 25.6 khz was repeatedly analyzed for different amplitudes under 0.6205 MPa of brake pressure and a motor speed of 1100 rpm. Table 5 presents the results for dither amplitudes ranging from 50 to 250 N. Using an average of the T1 and T2 results a clear downward trend is present. Figure 44 is a plot of this average versus the normal dither force amplitude. These tests demonstrate that dither has a slightly larger effect with increasing dither amplitude.

Table 5 Torque Reduction Values for Variable Dither Force Amplitude

PZT Voltage	Dither Force (N)	Torque Impact
20	50	0.48 to -0.29 %
65	100	-0.32 to -0.49 %
100	150	-0.24 to -1.33 %
125	200	-0.89 to -0.61 %
150	250	-1.46 to -1.38 %

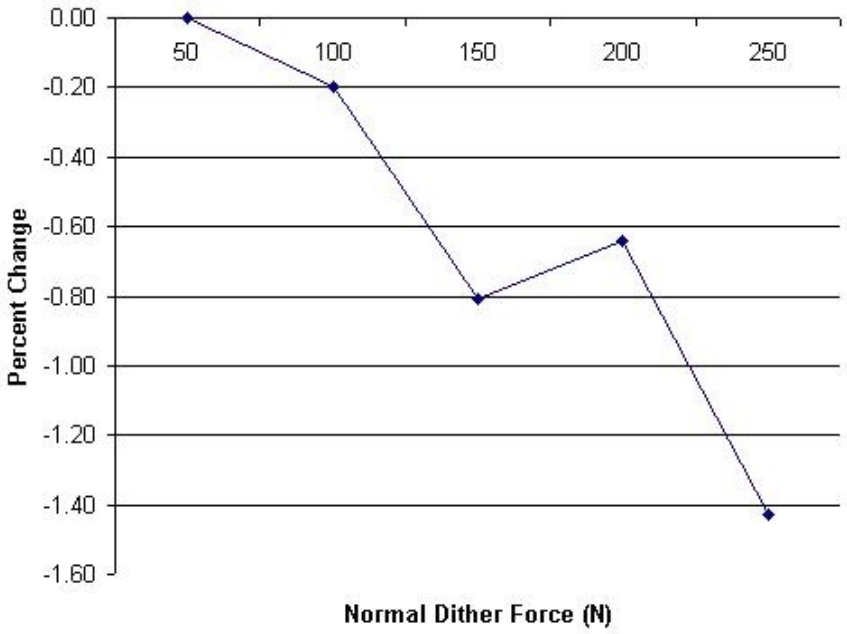

Figure 44 General Trend in Braking Torque Dependence on Dither Amplitude

4.6 Effect of Dither Control Frequency

The use of many dither frequencies greater than the squeal frequency was shown to effectively suppress brake squeal [1], therefore the relationship between torque impact and dither frequency becomes critical. To determine this effect ten different dither frequency signals were tested using a force amplitude of 200 Newtons under 0.6205 MPa of brake pressure and a motor speed of 1100 rpm. Five of these signals were chosen from the static transfer function response and five from the dynamic transfer function test. Table 4 presents the results for dither frequencies ranging from 2.9 kHz to 25.6 kHz. Using the same average of T1 and T2 as in the amplitude investigation, no clear trend is present. Figure 45 is a plot of this average versus dither frequency. These test demonstrate that the dither control frequency does not have a discernable pattern on the torque reduction in the brake system.

Table 6 Torque Reduction Values for Variable Dither Control Frequency

Frequency (khz)	Dither Force (N)	Torque Change	Average Torque Change (%)
2.9	200	-0.98 to –3.00 %	-1.99
4.5	200	-0.70 to -3.93 %	-2.32
4.6625	200	0.46 to -0.24 %	0.11
6.3	200	0.17 to -0.82 %	-0.32
11.3	200	-0.52 to -1.61 %	-1.06
12	200	-0.30 to -1.19 %	-0.74
18.66	200	-0.58 to -3.29 %	-1.93
19.25	200	-0.62 to -1.98 %	-1.30
24.5	200	-1.33 to -3.78 %	-2.55
25.6	200	-0.89 to -0.61 %	-0.75

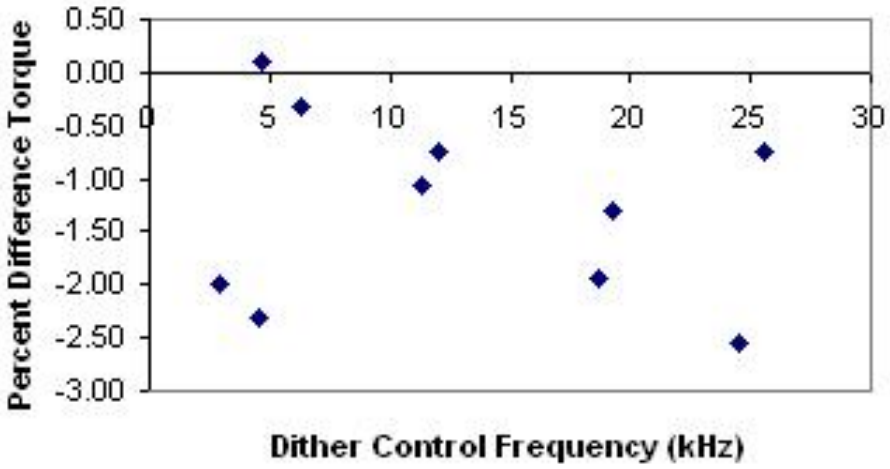

Figure 45 General Trend in Braking Torque Dependence on Dither Control Frequency

A closer look at the torque impact of the static frequencies and dynamic frequencies reveals that Hess and Soom's conclusion of greater torque impact near system resonance's is accurate. Figure 46 shows the average torque impact plot with a distinction between the two frequency types. Dither control frequencies that are associated with the primary resonances of the system (dynamic transfer function) have an

average torque change of –1.97 % while the static transfer function signals have an average torque change of –0.60 %.

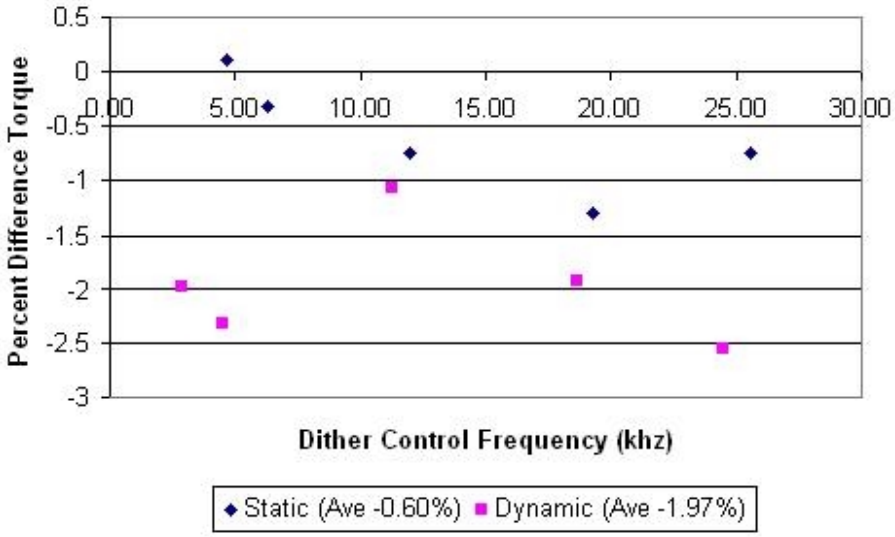

Figure 46 Comparison of Torque Impact of Excitation at Static vs. Dynamic Peak Response Frequencies

CHAPTER 5

CONCLUSIONS

The research presented here showed an experimental method of determining the effect of normal dither on effective braking torque. The results presented in the work at hand indicate that dither signal produces a slight reduction in the braking torque, no more than 1%. The experimental results fall between the predictions made by Ferri's friction model [12] and Hess and Soom's model [9-11]. These experiments also provide some light as to the nature of the squealing brake system and its relation to system vibration.

In many analytical and numerical simulations stability of the system or response of the system is used to quantify a squealing condition. In this research it was shown that the system does not vibrate at the squeal frequency when the brake is not squealing. This confirms the use of using system response as an indicator of squealing systems in numerical simulations. When comparing the vibration patterns of the rotor during squeal it is seen that squeal is a combination of several of the system's responses. It was also noted that the squeal response was influenced by boundary conditions (applied brake pressure).

Introducing a normal dither signal into a floating caliper brake system causes a small reduction in the braking torque. The reference dither signal caused a reduction in torque between –0.64 % and –0.88 %. Braking conditions had little to no effect on this result. Increasing the normal force amplitude increased the dither penalty on the system. This result is important since a threshold value of dither amplitude is necessary to obtain control of the system. The dither control frequency had a significant impact on torque results but provided no discernable pattern of change. Dither control frequencies chosen

from the dynamic (rotor in motion) transfer function had a greater impact on the system's braking torque than the dither control frequencies chosen using the static (rotor stationary) transfer functions.

REFERENCES

1. Graf, A., *Active Control of Automotive Disc Brake Rotor Squeal Using Dither*. 2000, MS Thesis The Georgia Institute of Technology.

2. ASME, *Research Needs and Opportunities in the Area of Interaction of Friction and System Dynamics*. 1994: Pittsburgh, PA.

3. Birch, T.W., *Automotive Braking Systems*. Third Edition ed. 1987, Marysville, California: Delmar Publishers.

4. Kinkaid N. M., O.R.O.M., Papadopoulos P., *Automotive Disc Brake Squeal: A Review.* Journal of Sound and Vibration, 2002.

5. Ouyang H., M.D., Brookfield J., James S., *On the stick-slip dynamics of an elastic slider on a vibrating disc.*

6. Matsuzaki, M. and T. Izumihara, *Brake Noise Caused by Longitudinal Vibration of the Disc Rotor*, in *SAE Paper 930804*. 1993.

7. Tuchinda A., H.N.P., Ewins D.J., Keiper W., *Mode Lock-in Characteristics and Instability Study of the Pin-On-Disc System.* 2000.

8. Oden, J.T. and J.A.C. Martins, *Models and Computational Methods for Dynamic Friction Phenomena.* Computer Methods in Applied Mechanics and Engineering, 1985. **52**(1-3): p. 527-634.

9. Hess, D.P. and A. Soom, *Normal Vibrations and Friction Under Harmonic Loads: Part I-Hertzian Contacts.* ASME Journal of Tribology, 1991. **113**(January): p. 80-086.

10. Hess, D.P. and A. Soom, *Normal Vibrations and Friction Under Harmonic Loads: Part II-Rough Planar Contacts.* ASME Journal of Tribology, 1991. **113**(January): p. 87-92.

11. Hess, D.P., A. Soom, and C.H. Kim, *Normal Vibrations and Friction at a Hertzian Contact Under Random Excitation: Theory and Experiment.* J. Sond Vib., 1991. **153**(3): p. 491-508.

12. Ferri, A.A., *Friction Damping and Isolation Systems.* ASME Journal of Vibration and Acoustics, 1995. **117B**(June): p. 196-206.

13. Tolstoi, D.M., *Significance of the Normal Degree of Freedom and Natural Normal Vibrations in Contact Friction.* Wear, 1967. **10**: p. 199-213.

14. Lee, S. and S.M. Meerkov, *Generalized Dither.* International Journal of Control, 1991. **53**(4): p. 741-747.

15. Pervozvanski, A., *Asymptotic analysis of the dither effect in systems with friction.* Automatica, 2001. **38**: p. 105-13.

16. Graf, A., *Experimental Active Control of Automotive Disc Brake Rotor Squeal Using Dither.* Journal of Sound and Vibration, 2002. **250**(4): p. 579-590.

17. Rye, R., *Investigation of Brake Squeal via Sound Intensity and Laser Vibrometry*. 2000, MS Thesis Georgia Institute of Technology.